Microcirculation in tissue repair: from microsurgery to 3D bioprinting

Matteo Amoroso

UNIVERSITY OF GOTHENBURG

Department of Plastic Surgery,
Institute of Clinical Sciences at Sahlgrenska Academy
University of Gothenburg

Gothenburg, Sweden, 2021

Cover and illustrations
by Matteo Amoroso

Microcirculation in tissue repair:
from Microsurgery to 3D bioprinting

matteo.amoroso@gu.se

ISBN 978-91-8009-144-2 (PRINT)
ISBN 978-91-8009-145-9 (PDF)

Printed in Borås, Sweden 2021
Stema Specialtryck AB

To My Wonderful Family.

Abstract

Microsurgical reconstruction is challenged by two main shortcomings: Perfusion Related Complication (PRC) and donor site morbidity. In the first 3 studies of this thesis, we aimed to provide solutions to PRC-problems, investigating hemodilution as a tool able to increase blood flow in flap microcirculation. In study I, we investigated the beneficial effect of hemodilution on the blood flow of a perforator free flap in a rat model and in study II, hemodilution was examined in a perforator pedicle flap. Overall, study I and study II showed that hemodilution improved flap survival. Study III, a systematic review of the current literature on hemodilution in microsurgery, demonstrated a lack of relevant clinical research on this topic in both clinical and experimental studies. The second part of this thesis aimed to investigate vascularization in 3D bioprinted constructs, a crucial step for bringing this technology into clinical practice, and thereby contribute to a solution to donor site morbidity. In both study IV (3D bioprinted microfractured fat) and V (3D bioprinted cartilage), the constructs were transplanted to nude mice and examined by longitudinal Magnetic Resonance Imaging, histology and immunohistochemistry. Results showed a perfusable vascular network growing around and into the constructs. In study IV, human blood vessels formed spontaneously from fragments of blood vessels in the lipoaspirate used for bioprinting. The blood vessels interconnected with the circulation of the host. In study V, the grid structure itself proved important for vascularization from the host. To summarize, this thesis shows that hemodilution could improve flap viability in microsurgical reconstructions but there is a lack of support for its effect in clinical studies. Vascularization of 3D bioprinted constructs can be achieved by printing with microfractured human fat. By printing in a gridded structure, vascularization can be further stimulated.

Keywords
Microsurgery, Hemodilution, Microcirculation, 3D bioprinting, Tissue regeneration

Sammanfattning på Svenska

Mikrokirurgiska rekonstruktioner begränsas av problem med blodcirkulationen i lambån och komplikationer från tagstället.I den första delen av detta avhandlingsprojekt undersöks om utspädning av blodet, hemodilution, kan påverka cirkulationen i lambån och om det finns stöd för att använda hemodilution i kliniken. I studie I studeras hemodilution i en råttmodell av fri mikrokirurgisk lambå och i studie II studeras effekten av hemodilution i en modell av stjälkad lambå på råtta. Studie I och II visar att hemodilution ökar överlevnaden av lambån genom ökad cirkulation. Studie III är en litteraturstudie av effekten av hemodilution i kliniska situationer och experimentella modeller. Studien visar att det saknas vetenskapligt stöd för att använda hemodilution i kliniken.

Den andra delen av avhandlingen syftar till att undersöka blodkärlsbildning i 3D bioprintad vävnad. Sådan vävnad kan bli ett alternativ för rekonstruktiv kirurgi och därmed bidra till att tagställesmorbiditeten minskar. Både studie IV (bioprintat fett) och V (bioprintat brosk) är experimentella studier där 3D bioprintat humant material transplanteras till immunoinkompetenta möss som sedan undersöks med magnetkamera. Preparaten undersöks efter försökets slut också med histologi och immunhistokemi.

Resultaten visar att ett nätverk av blodkärl växer runt om, och in i, de bioprintade vävnaderna och att blodkärlen kopplas samman med värddjurets cirkulation. I studie IV bildas mänskliga blodkärl spontant från blodkärlfragment som finns i fettaspiratet som används för att bioprinta. I studie V visas att porerna i den bioprintade vävnaden bidrar till blodkärlsinväxt.

Sammanfattningsvis visar studierna i denna avhandling att hemodilution förbättrar blodförsörjning i fria mikrokirurgiska och skaftade lambåer men att det saknas bevis för denna effekt i en klinisk situation. Kärlbildning av 3D bioprintad vävnad kan åstadkommas genom att printa med mikrofrakturerat fett som innehåller fragment av blodkärl och genom att printa med porer kan man stimulera blodkärlsinväxt i 3D bioprintad vävnad.

List of papers

This thesis is based on the following four papers, which will be referred to in the text by Roman numerals:

I. **Amoroso M**, Özkan Ö, Özkan Ö, Bassorgun CI, Ögan Ö, Ünal K, Longo B and Santanelli di Pompeo F. "The Effect of Normovolemic and Hypervolemic Hemodilution on a Microsurgical Model: Experimental study in Rats." Plast Reconstr Surg. 2015 Sep; 136:512-519

II. **Amoroso M**, Özkan Ö, Bassorgun CI, Ögan Ö, Ünal K, Longo B, Santanelli di Pompeo F and Özkan Ö."The Effect of Normovolemic and Hypervolemic Hemodilution on a Perforator Flap with Twisted Pedicle Model: Experimental study in Rats." Plast Reconstr Surg. 2016 Feb; 13:339e-346.

III. **Amoroso M**, Apelgren P, Elander A, Säljö K and Kölby L. "The effect of hemodilution on free flap survival: a systematic review of clinical and experimental studies." Clin Hemorheol Micro-circ. 2020 Vol.75(4), pp.457-466

IV. **Amoroso M**, Apelgren P, Säljö K, Montelius M, Strid Orrhult L, Engström M, Gatenholm P and Kölby L. "Vascularization of 3D Bioprinted Fat – Functional and Morphological Studies of Self-assembly of Blood Vessels." Submitted.

V. Apelgren P, **Amoroso M**, Säljö K, Montelius M, Lindahl A, Strid Orrhult L, Gatenholm P and Kölby L. "In Vivo MRI Reveals Functional Vascularization of Gridded 3D Bioprinted Cartilaginous Constructs." Submitted.

Contents

Abbreviations

ANH • Acute Normovolemic Hemodilution

AHH • Acute Hypervolemic Hemodilution

HCT • Hematocrit

Hb • Hemoglobin

BNC • Bacterial Nanocellulose

PRC • Perfusion Related Complication

PAD • Preoperative Autologous Donation

MRI • Magnetic Resonance Imaging

DWI-MRI• Diffusion-weighted magnetic resonance imaging

DCE-MRI• Dynamic contrast-enhanced magnetic resonance imaging

PFA• Paraformaldehyde

IS• Initial slope

AT• Arrival time

1. Introduction

1.1 Origin of Reconstructive Surgery

Reconstructive surgery aims to restore the human body in its "whole", both in form and function, following tumor extirpation, trauma or congenital or acquired deformity.

The roots of reconstructive surgery are as old as the "Sushruta Ayurveda", an ancient Sanskrit dated 600 BC, in which various surgical methods were first described. In Europe, the medieval surgeon Gaspare Tagliacozzi wrote De Curtorum Chirurgia per Insitionem in 1597 ("On the Surgery of Mutilation by Grafting") (Fig. 1).

Tagliacozzi describes, in great detail, the procedures and concepts that have bestowed upon him the honour of being one of the first plastic surgeons and his reconstructive approach is best explained by the below quote extracted from Tagliacozzi´s book:

"*We restore, rebuild, and make whole those parts which nature has given, but which fortune has taken away. Not so much that it may delight the eye, but that it might buoy up the spirit, and help the mind of the afflicted*" [1].

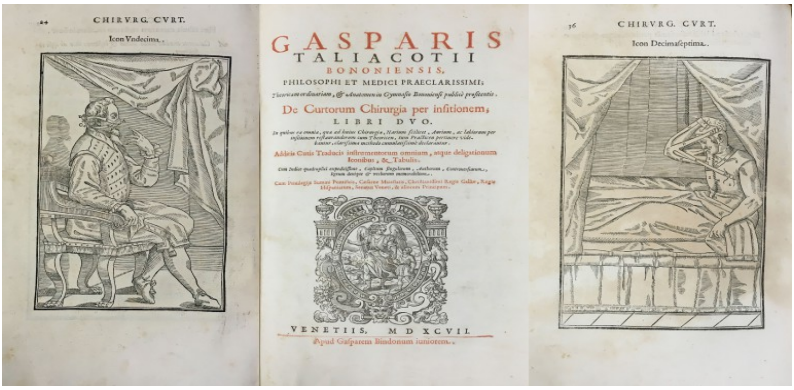

Figure 1. De Curtorum Chirurgia per Insitionem, 1597. Original illustration of the now-called "Italian method".

Until now, reconstructive solutions for tissue defects have relied on the use of autologous tissue (from the same individual), allogenic tissue (derived from a genetically different individual of the same species), alloplastic (artificial) implants, or a combination of these.

Although the above-mentioned reconstructive options are all effective, they have specific features and limitations [2] (Table 1).

Reconstructive option	Advantages	Disadvantages
Autologous	• No immunological complications • No ethical constraints • Biologically compatible • Fewer legal restrictions • No disease transmission	• Donor site morbidity • Limited quantity of tissue available • Greater risk and cost • Challenging harvesting cells in aged or diseased
Allogeneic	• No donor site morbidity • Donor cells may have higher viability • Tissue always healthy • Greater quantity of available tissue	• Temporary (e.g., cadaveric skin used in extensive burns) • Tissue typing is required • Immunosuppression may be needed • Risk of disease/rejection/death • Legal constraints • Ethical and psychological challenges
Alloplastic	• Maintain structural integrity • Predictable physical and mechanical properties • Cost effective • Avoids concerns over disease transmission	• Extrusion • Infection • Cannot restore all tissue/organ functions • Do not respond to biological cues/grow with patient • May provoke an immune/inflammatory/fibrotic reaction • Materials safety testing and manufacturing governance

Table 1. Advantages and disadvantages of different reconstructive options available in plastic surgery [2].

1.2 History of Microsurgery

The term Microsurgery find its origin in the Greek words "mikros" (meaning "small") and "skopein" (meaning "to view") and refer to surgery performed with the aid of a microscope.

Microsurgery allows transplantation of vascularized tissue (free flaps) from one part of the body to almost any other anatomic area. The first experimental free tissue transplantation was performed in a canine model based on the superficial epigastric vessels and published by Krizek et al. in 1965 [3].

The first successful human free flap was performed in 1970 in Oakland, California, by McLean and Buncke with use of the omentum for a large scalp defect [4], soon followed by transfer of the first composite flap, a groin flap, by Daniel and Taylor in January 1973 [5] and repeated 2 months later by O'Brien, both in Melbourne, Australia.

1.2.1 Evolution of microsurgical techniques.

The discovery that cutaneous tissue blood supply (Fig. 2) is based on small vessels called “perforating vessels “ led to the creation of fasciocutaneous flaps, as the forearm flap or Chinese flap [6].

Anatomical findings of perforator vessels in different regions of the body, led to the creation of several axial pattern flaps, e.g., the radial artery retrograde island flap, lateral crural flap and dorsalis pedis artery retrograde island flap, all described for the first time between 1980 and 1985. Taylor and Palmer, in 1987, described the location of perforator vessels throughout the entire human body [7]. The term "Perforator flap" was introduced by Isao Koshima in 1989 [8].

In the past decade, perforator flaps have increased significantly and their popularity is related to the accuracy in tissue type selection and the reduction of the donor site morbidity. Having their blood supply based only on the small perforator vessels, free or pedicled skin flaps can be elevated without disruption of muscular or fascial structures. The two most common examples are the antero lateral thigh flap (ALT) [9], typically used for oncologic head and neck reconstructions, and the deep inferior epigastric artery (DIEP) flap, used for breast reconstructions [10, 11].

Perforator based flaps can also be used as pedicled flaps. They are usually thin skin flaps based on a single perforator vessel, which is identified by Doppler. The perforator is then dissected down and isolated from the underlying feeding vessels. When the perforator flap is transferred through a rotational movement around its vascular pedicle, the flap becomes a "perforator propeller flap". These flaps are used when the perforator is located close to the defect and are particularly useful for reconstructions in the lower extremities.

Prefabrication of flaps

In areas where a particular shape, contour or framework is necessary and traditional methods cannot accomplish reconstructive objectives, prefabrication and prelamination strategies can be used [12, 13]

The flap prefabrication concept was introduced by Shen in 1982 [13]. It consists of a two-stage process involving the implantation of the main vascular pedicle in a selected donor site, followed by neovascularization of the flap during a period of about 8 weeks. This will allow transfer of the flap based on a new reliable vascular pedicle.

Flap prelamination, a concept invented in 1994 by Pribaz [11]. often applies to a two-stage procedure by which tissues grafted onto a vascular bed able to

supply a flap are transplanted "en bloc" with its original vascular supply. Commonly, these techniques become reconstructive options in response to demands for more sophisticated reconstructive efforts.

Supermicrosurgery

In 1997, Isao Koshima described perforator flaps based on vessels with diameters below 0.8 mm. One year later, the term "supramicrosurgery" was introduced in the description of a paraumbilical perforator flap [8]. Supermicrosurgical techniques allow anastomosis of vessels with diameters between 0.3 and 0.8 mm. This has led to the development of new reconstructive techniques such as the perforator-to-perforator flaps, in which the pedicle is divided above the fas-cia. This technique truly minimizes donor site morbidity because the fascia re-mains intact.

To date, the introduction of supermicrosurgical anastomosis allowed the use of different flaps harvested from the lateral thoracic wall, paraumbilical and thigh as well as in the gluteal and groin areas [14].

In recent years, the Taiwanese microsurgeon Fu-Chan Wei presented a new approach to perforator flap surgery [15]. This technique is also called free-style approach, since it permits harvesting of very thin flaps, by dissecting only the most superficial perforators and in a free-style manner. A Doppler probe is used, often intraoperatively, to identify the location of the perforating vessel and the free-style flap can be thus be designed in almost any part of the body.

1.2.2. Development of clinical application of Microsurgery

Transplantation of free vascularized tissue allows coverage of complex defects with many tissue types, including bone and nerve with sensate skin thus allowing

reconstructions with functioning tissues. In hand surgery, replantation became the first clinical application of microvascular surgery, making digital replantations possible, first performed by Tamai in 1965 [16].

Oncologic reconstruction is another area that has been transformed by microsurgery. Defects that in the past could only be reconstructed by skin grafts or pedicled flaps, can now be reconstructed with well-tailored, vascularized segments of tissue that can include several tissue types including skin, fat, fascia, muscle and bone. Perhaps this is best emphasized in the head and neck area where local tissues are often limited, and the ability to bring in well-vascularized tissue of the correct size, shape and type is critical for both appearance and function [17].

Microsurgery has also improved the treatment of complex open fractures and surgical infections. In the past, advanced tibial osteomyelitis often resulted in amputation. With the introduction of free muscle flaps, a thorough excisional debridement and subsequent coverage with a sizeable free muscle flap and later bone grafting can result in both cure and limb salvage [18].

1.3 Main limitations in Reconstructive Microsurgery

Despite the technical improvements and refinements, microsurgical reconstructions remain limited by two main aspects:

1) Complications associated to inadequate flap perfusion also defined as perfusion related complications (PRC) [19] resulting in flap necrosis and consequent total or partial loss of the flap.

2) Donor site morbidity associated with autologous tissue harvest as well as the finite availability of suitable tissue to be transplanted [19-22].

1.3.1 Perfusion Related Complications (PRC)

PRC are complications associated with inadequate flap perfusion [19] resulting in flap necrosis and consequent total or partial loss of the flap. PRC can be the result arterial thrombosis, venous thrombosis, or even the distribution of the vascular system in relation to the flap area.

1.3.2 Donor Site Morbidity

The incidence of donor site complications varies between 5.5% and 31%. Early donor problems are associated with wound healing, e.g. hematoma, seroma and wound dehiscence [23]. Hematoma formation can occur with any flap; large dead spaces like the latissimus dorsi donor site are especially susceptible to seroma formation. Wound dehiscence occurs with tight closure, typically with the DIEP, TRAM, gracilis, scapular and dorsalis pedis flaps [21, 23]. Long-term morbidity includes problems with form, function or pain and a cosmetic defect [23, 24]. A prospective study of 100 patients with radial forearm flaps showed delayed healing in 22% of the patients and tendon exposure in 13% [25]. Irrespective of whether the tissue for reconstruction is harvested loco-regionally, or remote, the supply is limited and some degree of donor site morbidity is inevitable.

1.4 Hemodynamics in free flaps

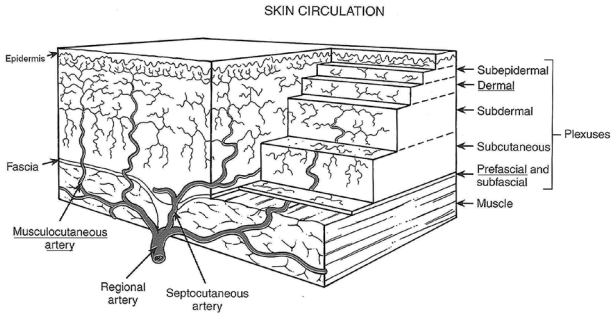

Figure 2. Blood vessel distribution of the skin [26].

Blood flow is determined mainly by two factors: 1) the pressure gradient from one point to another in a vessel, and 2) the vascular resistance [27].

The French physician, Poiseuille was the first to relate the blood viscosity to the capillary system blood flow. He described with a formula the laminar flow of a fluid through a straight cylindrical tube. The formula describes how the flow is related to perfusion pressure, radius, length, and viscosity (Fig. 3).

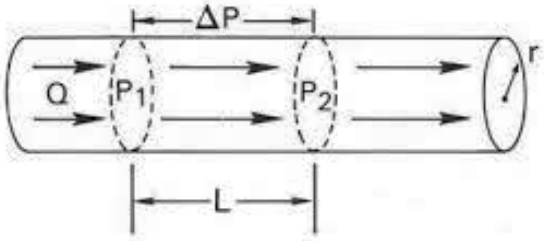

Figure 3. Poiseuille's equation, $F = \Delta P\ \pi\ r^4 / 8\ L\mu$, applied to a circular pipe. F is flow, ΔP is perfusion pressure (pressure difference between the two ends of a tube), r is the radius, L is length and μ is viscosity

As the cross-section increases, the blood velocity decreases. The vessel radius appears in the equation at the fourth power and represents the parameter whose variations affect the flow the most. Newton's Law of Friction defines viscosity. The tangential force of friction opposes the sliding of two sheets of liquid adjacent to each other. The blood viscosity (μ) represents the resistance, measured in poise [28]. The viscosity of blood is closely related to the blood flow velocity and the hematocrit (HCT), a blood measurement unit indicating the volume fraction of blood occupied by red blood cells. HCT is generally between 41%-50% in men and 36%-48% in women. The viscosity of the blood increases as the HCT increases. The increase in viscosity (for example in polycythemia) causes an increase in resistance to flow, with a consequent increase in cardiac work. Conversely, viscosity tends to be reduced in an anemic state.

When HCT is reduced in a linear controlled fashion, systemic oxygen transport first increases, reaches a peak value at 30 % HCT, and falls to insufficient critical levels when the HCT reaches values lower than 20 %. When HCT increases to over 40 %, the viscosity increases dramatically and leads to a viscosity-dependent drop in capillary perfusion [27, 29, 30]. In the microcirculation, viscosity undergoes further modification and the diameters of capillary blood vessels regulate the blood supply to the flap. The blood viscosity decreases with the calibre of the vessel due to the so called “Fahraeus-Lindqvist effect” (Fig 4). The red blood cells dispersed in a fluid, which flows with laminar motion at a sufficiently high speed, are pushed towards the vessel's central axis, where the sliding speed is higher, causing accumulation of red blood cells in the center of the vessel (axial accumulation). Consequently, the relative viscosity of the blood is higher in the center of the vessel (high HCT) and lower in the periphery. The phenomenon is observed for calibers smaller than 300 μm (arterioles). The apparent viscosity tends to increase again in vessels with a diameter close to that of red blood cells (7-8 μm) [29].

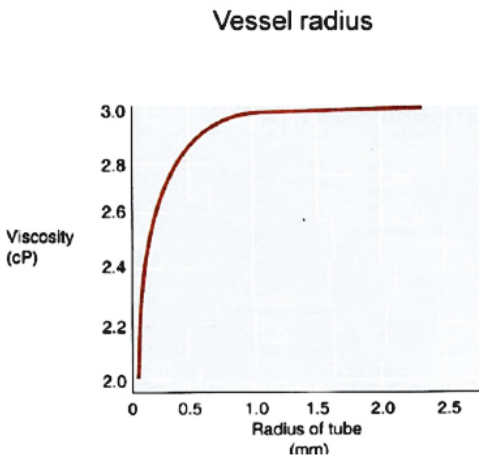

Figure 4. Relationship between blood viscosity and blood vessel caliber.

1.4.1. Factors decreasing blood flow in free flaps

Hypothermia may mimic decreased flap perfusion. Moreover, it may instigate arterial spasm, decreasing flow to the flap, and initiating a thrombotic cascade. Systemic hypotension can cause decreased flap perfusion due to decreased intravascular volume and a decrease in perfusion pressure. Cardiac output is volume dependent, and hypovolemia results in reduction of cardiac preload and subsequently reduction of cardiac output that, in turn, further increase the vascular resistance. As a consequence of increased vascular resistance, red blood cells (RBC) may stack, forming chains of agglomerated RBC, so called "rouleaux formation" [31].

When vessels are cut and transferred, they are essentially sympathectomized. This leads to loss of vascular tone and decreased resistance. Sympathectomy relieves arteriolar vasoconstriction leading to increased perfusion in the entire flap [32-34]. Vasodilation is also due to loss of muscular tone after denervation.

Therefore, preference should be given to volume repletion over the administration of sympathomimetic drugs by the anesthesiologist to restore normotension [28]. There are many reasons that the flow in a free flap is not similar to the flow in the same intact pedicle. First, all minor vessels are divided and all blood flow is through the anastomosed vessel. On the other hand, vasoconstriction should always be taken into account [31]. The dissection of the pedicle, or hypothermia, may result in vasospasm.

1.4.2 Effect of different interventions on blood flow in the flap

A variety of pharmacologic agents have been used attempting to improve blood flow in flaps with limited effect on flap blood flow [35]. In the perioperative period there are several factors could potentially influence the outcomes in free tissue transfer. Motakef et al in 2014, published a systematic review of the literature to identify strategies that could guide perioperative management, improve outcomes and minimize complication of free tissue transfer [36] but to date, there has been a lack of reliable evidence to guide such perioperative management.

1.4.3 Effect of hemodilution on free flaps

Acute Normovolemic Hemodilution (ANH) [37] has been proposed to improve blood perfusion in transplanted tissue [31, 38-41]. Studies have shown that reduction of the systemic HCT induced by ANH is associated with a reduction in blood viscosity and red blood cell shear stress, thereby increasing blood perfusion in free tissue transfer [31, 38-41] . ANH and Acute Hypervolemic Hemodilution (AHH) have been shown clinically and experimentally to have a beneficial effect on tissue perfusion in ischemic conditions [31, 42].

Hemodilution can be achieved in several ways. First, by pre- or perioperative withdrawal of blood with simultaneous infusion of plasma substitutes (normovolemic hemodilution). Second, by infusion of fluid (hypervolemic hemodilution). It has been suggested that during hemodilution, the average capillary HCT falls less than the systemic HCT, and red blood cells are distributed more homogeneously. Both effects are supposed to improve tissue oxygenation [31]. The use of ANH has been reported in craniosynostosis surgery and in neurosurgical procedures and is claimed to give a clinically relevant benefit [43]. The decrease in blood viscosity following hemodilution generate a uniform distribution of oxygen in the tissues. Therefore, hemodilution could possibly generate the same benefit when applied to microvascular reconstructions [28, 31, 39-41, 44-46].

Moreover, the use of hemodilution and postoperative autologous blood transfusion would prevent the need for unnecessary allogeneic blood transfusions. Despite that, the literature concerning the use of hemodilution for preventing perfusion complications in perforator free flap is limited and controversial, both in clinical and experimental studies. This is the background and rationale for the studies behind study I, II and III of the present thesis.

1.5 3D bioprinting in reconstructive surgery

The 3D bioprinting is a technology characterized by the unique ability of generate living tissue by its ability to print 3D structures using multiple cell types, biomaterials, and biomolecules in a layer-by-layer fashion [47].

1.5.1 Bioprinting techniques

The three major bioprinting methods are: inkjet bioprinting, extrusion bioprinting and laser-assisted bioprinting (Fig. 5). Each has specific strengths, weaknesses, and limitations.

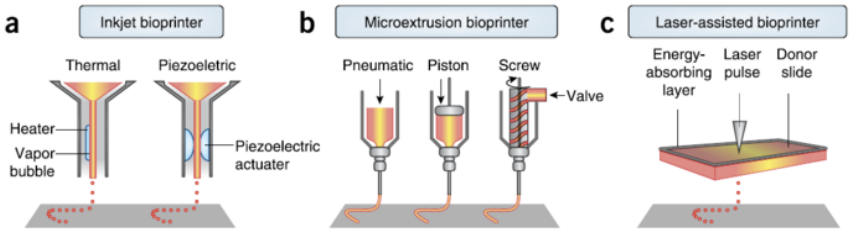

Figure 5. Schematic illustration of 3D bioprinting: a) inkjet bioprinting, b) extrusion bioprinting and c) laser-assisted bioprinting [48].

Inkjet bioprinting

Inkjet bioprinting was the first bioprinting technology [49]. Cells and bioink are mixed in a cartridge and printed by aggregation of droplets. The technique is relatively cheap and fast. One drawback is its limited ability to print with high-viscosity (cell-dense) inks [50, 51].

Microextrusion bioprinting

Microextrusion bioprinters are the least expensive and therefore common [52]. A microextrusion bioprinter ejects microbeads of bioinks pneumatically or mechanically. On advantage of microextrusion inkjet printing is the ability to print

high-viscosity (cell-dense) bioinks. However, they expose the printed cells to mechanical stress reducing cell viability [48].

Laser-assisted bioprinting

Laser-assisted bioprinting prints with very high resolution and has minimal negative effect on the printed cells. However, the technique is slow [53-55].

1.5.2 Bioink

The composition of the bioink used in 3D bioprinting is important. The most obvious requirement is biocompatibility, defined as "the ability of a material to perform with an appropriate host response in a specific application" [56].
Hydrogels represent the main material used for bioink. Hydrogels can be synthetic, e.g. PEG-based (poly-ethylene glycol), or based on natural polymers like nanocellulose, collagen, hyaluronic acid, chitosan or alginate. The high water content makes them similar to extracellular matrix [54, 57-61]. However, their viscoelastic properties counteract printing with good resolution [62]. Moreover, their mechanical properties are not adequate for clinical applications. Differently, the nanocellulose-alginate bioink provides a biologically appropriate environment and has excellent high resolution printing properties, which makes it a promising material for clinical applications.

1.5.3 3D bioprinting of human adipose tissue

The Clinical problem.

Soft-tissue defects represent a challenging problem to solve and suboptimal strategies are available. At present, treatment of large

volume defects includes the use of free flaps. For smaller defects, free fat grafting is often the method of choice [63].
Free flaps may suffer from PRC and donor site morbidity and free fat grafting suffer from unpredictable reabsorption [64, 65]. Engineered tissues could reduce the scarcity of native autologous fat and do not lead to donor site morbidity [66].

1.5.4 3D bioprinting of human cartilage tissue

The clinical problem.

Cartilage defects are common and challenging [67]. Reconstruction of e.g. the external ear is based on old techniques dating back to 1959 [68]. However, this method suffers from limitations such as limited source of tissue, poor cosmetic results and donor site morbidity [69, 70].

3D bioprinting technology could possibly bridge these reconstructive processes using autologous chondrocytes mixed with a biomaterial which then can be printed in the desired shape.

Several different approaches have been explored including altering scaffold geometry and porosity [71-77], incorporation of biomimetic vessels and endothelial cells, smooth muscle cells as well as addition of growth factors [78-81]. Even if cartilage is avascular in itself, blood vessels are needed to be able to create larger viable implants and these vessels somehow need to be connected to the systemic circulation [82, 83].

1.5.5 Vascularization limits 3D bioprinting

3D printed grafts generally lack vascularization. They are therefore severely restricted in size since they rely on diffusion to provide oxygen and nutrients to the incorporated cells [84-90]. The diffusion range is about 200-250 μm, and a construct depending totally on diffusion could therefore not be thicker than 0.5 mm [91, 92]. The presence of a microvascular network remains necessary to guarantee the metabolic needs of the 3D bioprinted tissue [84-90] and represents the most critical obstacle for 3D bioprinted constructs to become clinically relevant [93, 94].

The scaffold design and architecture are proposed as tools to improve vascularization in engineered constructs. The pore size of the scaffold and their interconnectivity have a significant effect on vascularization rate and cell growth [88, 92]. One strategy to overcome this limitation is printing a construct with a gridded architecture [92]. An investigation of the effect of a gridded structure is the basis for study V of the present thesis. A further investigation of the vascularization of printed fat constructs is the basis for study IV of the present thesis.

1.5.6. MRI studies: DCE-MRI and DW-MRI techniques

MRI-based techniques are widely employed to assess perfusion and diffusion properties of various native tissues [95]. The non-invasiveness of MRI techniques make them clinically relevant and suitable tools for in vivo assessment of tissue perfusion and diffusion properties. Dynamic contrast enhanced MRI (DCE-MRI) provides reliable information on tissue perfusion. After an intravenous injection of contrast agent, the MR signal increases in proportion to the contrast agent concentration in a specific voxel (volume pixel). By studying the voxel signal behavior before, during, and after contrast administration, we can obtain semiquantitative parameters characteristics of the perfusion like the arrival time (AT) and initial slope (IS). The arrival time (AT), is the time between the injection of the contrast agent into the animal and arrival in the construct. Short AT values denote an effective vasculature and vice versa. Using color coded AT values, functional maps can be generated, providing semiquantitative visual information on the different AT values distribution in the area of interest. The ground principle of Diffusion-weighted MRI (DWI-MRI) technique relates to the transportation of nutrients and oxygen from the vascular structures to the cells which relies on passive diffusion through the extracellular space.

AIMS

The research project presented in this thesis is organized in 2 main parts: *i.* studies on microcirculation in flaps and *ii.* studies on microcirculation in 3D bioprinted tissues.

The aims of this thesis are:

1. To determine the effect of ANH and AHH on microcirculation and flap survival of a free flap
2. To determine the effect of ANH and AHH on microcirculation and flap survival of a twisted flap
3. To determine the level of evidence for the effect of ANH and AHH in clinical and experimental models
4. To study the perfusion and diffusion in 3D bioprinted fat and thereby determine if spontaneous vascularization plays a role for the transport of oxygen and nutrients in the constructs
5. To study the perfusion and diffusion in 3D bioprinted cartilage thereby determine if a gridded structure plays a role for vascularization

2. Methodological considerations

2.1.1 Study design (Study I-II)

In study I, we investigated the potentially beneficial effect of hemodilution on the microcirculation in free perforator flaps in a microsurgical rat model. In study II, we further investigated the effect of hemodilution on the microcirculation in pedicled perforator flaps in a rat model. The flap pedicle was twisted to different degrees of rotation (90, 180, 270, and 360 degrees). Approval for the both studies was obtained from the Animal Care Committee, Akdeniz University, Antalya, Turkey.

In study I, forty female Wistar rats weighing 204.0 ± 16.5 (mean ± SD) g were allocated randomly into four groups of 10 rats each. In group 1 (Control), a superficial inferior epigastric artery (SIEA) flap was raised and the pedicle dissected until reaching the femoral vessels which were isolated, sectioned, and the stumps anastomosed without performing hemodilution. In group 2, ANH was performed 24h before surgery. In group 3, AHH was performed 24h before surgery. In group 4, we raised the SIEA flap and ligated the femoral artery and vein, proximal to the flap perforator, to validate the microsurgical model used, excluding the presence of a distal reverse reflow in the flap.

In study II, sixty-three female Wistar rats weighing 202.0 ± 13.6 g were allocated randomly into three main groups of 21 animals each. In all rats, two SIEA flaps were raised, one from each side of abdomen, and transposed back with different degrees of rotation (90, 180, 270, and 360 degrees). In addition, in one animal in each group the two flaps were sutured back without rotation. In group 1 (Control), only surgery was performed. In group 2, ANH was performed 24 h before

surgery. In group 3, AHH was performed 24 h before surgery. Five distinct subgroups were thus created depending on the 5 different degrees of rotation of the flap pedicle as summarized in Table 2. In subgroup 1 the flap was rotated 90 degrees. In subgroup 2 rotation was 180 degrees. In subgroup 3 the rotation was 270 degrees. In subgroup 4 the rotation was 360 degrees.

Two flaps with 0 degrees of pedicle rotation were also performed in every main group (subgroup V).

Groups	**Subgroups**	**1**	**2**	**3**	**4**	**5**		
	No. of animals and flaps	**90º**	**180º**	**270º**	**360º**	**0º**	**Total no. of animals**	**Total no, of flaps**
CONTROL	**Animals**	**5**	**5**	**5**	**5**	**1**	**21**	
	Flaps	**10**	**10**	**10**	**10**	**2**		**42**
ANH	**Animals**	**5**	**5**	**5**	**5**	**1**	**21**	
	Flaps	**10**	**10**	**10**	**10**	**2**		**42**
AHH	**Animals**	**5**	**5**	**5**	**5**	**1**	**21**	
	Flaps	**10**	**10**	**10**	**10**	**2**		**42**
Total no, animals		**15**	**15**	**15**	**15**	**3**	**63**	
Total no, flaps		**30**	**30**	**30**	**30**	**6**		**126**

Table 2. The distribution of flaps with different degrees of rotation in study II. Each main group consisted of 21 animals and 2 flaps were raised on each animal.

2.1.2 Hemodilution technique (Study I-II)

Anesthesia was performed by intraperitoneal injection of ketamine (90 mg/kg) plus xylazine (10 mg/kg).

In study I, hemodilution was obtained using the femoral artery contralateral to the flap (Fig. 6A). A permanent arterial catheter (2-French, 0.7-mm external diameter, 80-mm length) was placed in the femoral artery and tunneled to a subcutaneous pocket on the back of the animal (Fig. 6B) for blood pressure measurement, blood sampling and blood removal during the hemodilution.

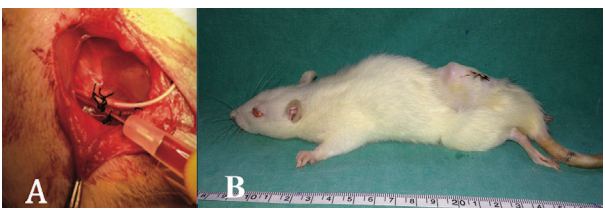

Figure 6. A) Hemodilution technique. Acute normovolemic hemodilution was obtained by removing the desired amount of blood through the permanent catheter placed into the femoral artery and simultaneously replacing the blood removed with isotonic 0.9% sodium chloride plus 6% hydroxyethyl starch using the catheter placed in the femoral vein. B) After hemodilution, the permanent arterial catheter was tunneled subcutaneously, placed in a pocked on the back of the animal and used for blood pressure measurements and blood samples.

With 2 infusion pumps, ANH was achieved by simultaneous extraction of the required quantity of blood (mean 2.25 ml) from the femoral artery catheter and replacing it with an equal volume of a mixture composed by two thirds of 0.9 % isotonic sodium chloride and one third of 6 % hydroxyethyl starch, infused in the femoral vein to maintain normovolemia. To calculate the amount of blood volume to be exchanged to reach the desired HCT value, the Gross equation was used: V = EBV x [(Ho − Hf)/ Hav], where, EBV is the total blood volume, Ho

is the initial HCT, Hf is the minimum allowable HCT, and Hav is the average of the initial and minimum allowable HCT.

AHH was obtained by performing an ANH as described above followed by an extra infusion of liquid equivalent to 20 % of the total blood volume. AHH induces a reduction of the HCT level and hypervolemia.

In study II, the common carotid artery and the tail vein were used as arterial and venous access. A permanent arterial catheter (2-French, 0.7-mm external diameter, 80-mm length) was placed in one common carotid artery and tunneled to a subcutaneous pocket on the back of the animal to be used for blood pressure measurement, blood sampling and blood removal during the hemodilution (Fig. 7).

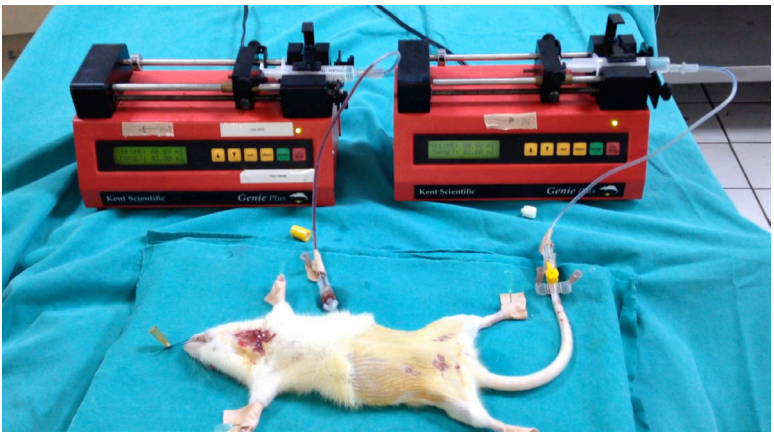

Figure 7. Acute Normovolemic Hemodilution was obtained using two infusion pumps, simultaneously removing the desired amount of blood through a catheter placed into the common carotid artery and replacing the blood removed with a mixture colloid/crystalloid from the tail vein.

2.1.3 Experimental animal model (Study I-II)

In study I, one SIEA flap was raised in all animals 24h after the hemodilution process. The skin paddle of the SIEA flap measured 4 x 4 cm and was raised at the subpannicular level. The superficial inferior epigastric perforator was located and followed to the femoral vessels. The femoral vessels (artery and vein) were isolated and sectioned. Microvascular anastomoses were performed under the microscope using 10-0 nylon interrupted sutures. The anastomoses were observed under the microscope for 15 minutes and a patency test was performed (Fig. 8). After revascularization, the flap was sutured to its original location with 5-0 monofilament nylon sutures.

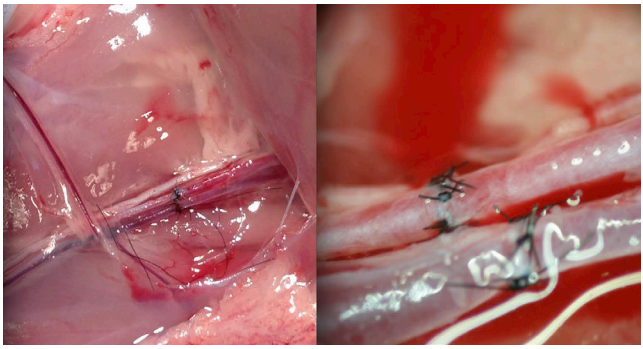

Figure 8. (Left) The femoral vessels and the superficial inferior epigastric vessels were identified, and the flap was elevated. (Right) The femoral artery and vein were isolated and sectioned, and microvascular anastomoses were performed under the microscope using 10-0 nylon sutures.

In study II, two separate SIEA flaps measuring 4 x 4 cm were elevated on all animals. The SIEA flaps was designed bilaterally on the animal abdomen, with the medial margin of this skin flap located on the abdominal midline. The flap was elevated at the subpannicular level, and the superficial inferior epigastric perforator was identified and followed to the femoral vessels. The pedicle was

isolated to remove minor blood vessels and perivascular tissue that could potentially nourish the flap. The flaps were twisted around its pedicle with different degrees of rotation (0, 90, 180, 270 ,360 degrees) and then sutured back in their original position with 5-0 monofilament nylon (Fig. 9).

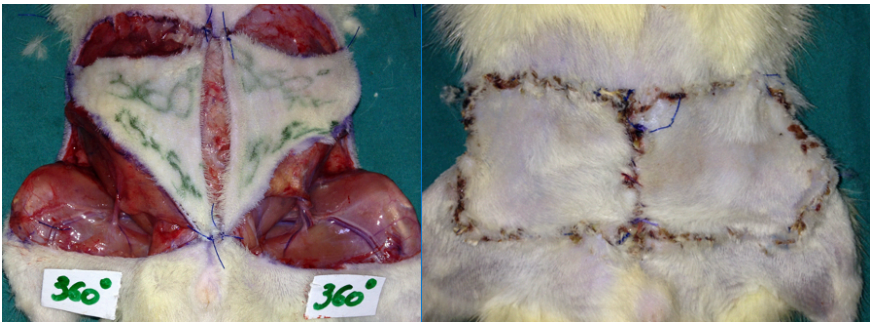

Figure 9. (Left) Intraoperative view. The flaps were designed bilaterally on the abdomen in a square shape. The flap was raised and the perforator identified and followed until its origin to the femoral vessels. (Right) The flap was sutured back in its original position after a 360-degree rotation around its vascular pedicle.

2.1.4 Direct observations (Study I-II)

After 7 days, photos of all flaps were taken and the viability was determined by the clinical evaluation of flap color, hair growth, and necrotic skin areas. Pictures were then analyzed using Adobe Photoshop CS 5 software (Adobe Systems, Inc., San Jose, Calif, USA) to determine the percentage of viable flap and skin necrosis. The viable areas in each flap were then expressed as a percentage of the total flap surface area.

2.1.5 Histological analysis (Study I-II)

The entire flap and the middle portions of the pedicle were excised separately and fixed in formalin for histopathologic examination with standard hematoxylin and eosin (H&E) staining.

2.1.6 Microangiography (Study I-II)

Microangiography visualized the overall perfusion in the flaps and outlined the architectural differences between the different groups. This was achieved by injecting radiopaque contrast through the common carotid artery. About 20 – 25 ml of a 30% solution of lead oxide (Micropaque; Guerbet, Bloomington, Ill, USA) was used per animal. The lead oxide infusion was stopped when the contrast began to ooze from the edges of the flap. The flaps were then resected and stored in a refrigerator at 4°C for 24 hours and the examined by radiography with a soft x-ray machine (Mammo Diagnost UC; Philips, Hamburg, Germany) at settings of 24 kV and 10 mA, using Microvision-C (DuPont, Wilmington, Del, USA) mammography film. The images were analyzed using Adobe Photoshop CS 5 software. The assessment of the vascularized areas in the images obtained were highlighted and defined by the contrast agent infused and manually outlined and then measured by using the histogram function. To assess the number of pixels detected, the pixel measurement function in Photoshop CS5 and the total number of pixels detected in the outlined areas were used to compare the degree of vascularization.

2.1.7 Statistical Analysis (Study I-II)

In study I, a two-tailed t-test was performed on the HCT values of groups 1, 2, and 3. Analysis of variance (ANOVA) was conducted among the groups to establish the statistical significance difference in terms of flap survival (%) between the three different groups. In study II, we performed a two-tailed t-test to analyze the HCT values and ANOVA was used for the flap survival. Furthermore, Bonferroni adjustment was done to compensate for multiple comparisons.

2.2.1 Search methods (Study III)

We performed a systematic search analysis of the available literature of both clinical and experimental articles addressing the impact of hemodilution on free flap viability.

This was achieved with a specific search string applied to the following scientific databases: Medline, Google Scholar and ClinicalTrials.gov. In order to improve the accuracy of our analysis, it was conducted following the guidance of the Preferred Reporting Items for Systematic Reviews and Meta-Analyses (PRISMA) statement [96] and the Cochrane handbook for systematic reviews of interventions [97]. The searching process was performed in a time interval between January 2017 and January 2019. The analysis was carried out without restriction related to the language or publication status of the articles encountered. The patient, intervention, comparison, outcome (PICO) model was used for the evaluation of studies' eligibility for inclusion in the review [98]. In the review, we included only peer-reviewed articles having a study population undergoing microvascular reconstructive surgery and in which hemodilution treatment was applied. Articles investigating an anemic state, not induced by hemodilution treatment, as well as studies in which interventions other than hemodilution were used, were excluded. The PICO method was adopted for the assessment of both experimental and clinical studies (Table 3).

Parameters	Inclusion criteria	Exclusion criteria
Patients	Patients undergoing microvascular reconstruction and receiving hemodilution treatment versus any other treatment or placebo.	Patients undergoing other types of surgery different from a microsurgical free tissue transfer
Intervention	ANH treatment	Lack of ANH as intervention
Comparator	Effectiveness of ANH compared to any other treatment, placebo or control.	
Primary Outcomes	The rate of total flap failure, defined by complete flap loss. The rate of partial flap failure, defined by either partial skin flap necrosis, fat necrosis or complication related to the insufficient flap perfusion	
Secondary Outcomes	Medical complications: Death, myocardial infarction, stroke, and pulmonary complication (pneumonia, atelectasis, and pulmonary edema)	

Table 3. PICO criteria for inclusion and exclusion of studies [98].

2.2.2 Study selection and data extraction (Study III)

Two researchers (M.A. and L.K.) individually reviewed all abstracts and titles encountered. The complete text of the paper was then assessed and the eligibility validated using the PICO method. A third reviewer was involved if disagreement occurred between the first 2 reviewers. The following information were extracted from the selected articles: author(s), year of publication, number of flaps, time of intervention, amount of blood withdrawn, rates of flap necrosis as well as total flap loss.

2.2.3 Risk of bias and quality assessment (Study III)

Assessment of the risk of bias in the animal studies was conducted using the Systematic Review Centre for Laboratory Animal Experimentation Risk of Bias (SYRCLE RoB) tool [99]. This method detects aspects of bias specific for

experimental animal studies (Table 4) [99]. The Grading of Recommendations Assessment, Development, and Evaluation (GRADE) system was used to examine the treatments and interventions in the selected studies in order to assess the level of evidence and quality of the included studies [100] (Table 5).

Table 4. The SYRCLE RoB tool for assessing risk of bias [99].

Item	Type of bias	Domain	Description of domain	Review authors judgment
1	Selection bias	Sequence generation	Describe the methods used, if any, to generate the allocation sequence in sufficient detail to allow an assessment whether it should produce comparable groups.	Was the allocation sequence adequately generated and applied? (*)
2	Selection bias	Baseline characteristics	Describe all the possible prognostic factors or animal characteristics, if any, that are compared in order to judge whether or not intervention and control groups were similar at the start of the experiment.	Were the groups similar at baseline or were they adjusted for confounders in the analysis?
3	Selection bias	Allocation concealment	Describe the method used to conceal the allocation sequence in sufficient detail to determine whether intervention allocations could have been foreseen before or during enrolment.	Was the allocation adequately concealed? (*)
4	Performance bias	Random housing	Describe all measures used, if any, to house the animals randomly within the animal room.	Were the animals randomly housed during the experiment?
5	Performance bias	Blinding	Describe all measures used, if any, to blind trial caregivers and researchers from knowing which intervention each animal received. Provide any information relating to whether the intended blinding was effective.	Were the caregivers and/or investigators blinded from knowledge which intervention each animal received during the experiment?
6	Detection bias	Random outcome assessment	Describe whether or not animals were selected at random for outcome assessment, and which methods to select the animals, if any, were used.	Were animals selected at random for outcome assessment?
7	Detection bias	Blinding	Describe all measures used, if any, to blind outcome assessors from knowing which intervention each animal received. Provide any information relating to whether the intended blinding was effective.	Was the outcome assessor blinded?
8	Attrition bias	Incomplete outcome data	Describe the completeness of outcome data for each main outcome, including attrition and exclusions from the analysis. State whether attrition and exclusions were reported, the numbers in each intervention group (compared with total randomized animals), reasons for attrition or exclusions, and any re-inclusions in analyses for the review.	Were incomplete outcome data adequately addressed? (*)
9	Reporting bias	Selective outcome reporting	State how selective outcome reporting was examined and what was found.	Are reports of the study free of selective outcome reporting? (*)
10	Other	Other sources of bias	State any important concerns about bias not covered by other domains in the tool.	Was the study apparently free of other problems that could result in high risk of bias? (*)

*Items in agreement with the items in the Cochrane Risk of Bias tool.

Quality of evidence	Definition
High	We are very confident that the real effect lies close to that of the estimate of the effect
Moderate	We are moderately confident in the effect estimate: The real effect is likely to be close to the estimate of the effect, but there is a possibility that it is substantially different
Low	Our confidence in the effect estimate is limited: The true effect may be substantially different from the estimate of the effect
Very low	We have very little confidence in the effect estimate: The true effect is likely to be substantially different from the estimate of effect

Table 5. GRADE analysis and definition [100].

2.3.1 Experimental design (Study IV-V)

In studies IV and V, 3D bioprinted constructs with human cells (human micro-fractured fat in study IV and human nasal chondrocytes in study V) were subcutaneously allocated on the back of nude mice. Animals in the control group received cell-free constructs. The animals underwent MRI examination with intravenous injection of contrast agent at four sequential timepoints after implantation; timepoint 1 (0-3 days), timepoint 2 (7-9 days) timepoint 3 (8-29 days) and timepoint 4 (97-99 days), respectively. Following the final MRI, the animals were sacrificed. The study was approved by the Ethics Committee for animal experiments at Sahlgrenska University Hospital (University of Gothenburg, Göteborg, Sweden, Dnr 119–2015).

2.3.2 Cell source (Study IV-V)

In study IV, waste adipose tissue obtained through liposuction was collected from a healthy female donor with approval from the Regional Ethics Committee of Gothenburg (Dnr 624-16). In short, lipoaspirate was washed in 0.9 % NaCl, emulsified by shaking with metal beads 4 x 30 s, and rinsed in a closed system.

In study V, human nasoseptal chondrocytes (hNCs) from four male donors were cultured under standard culture conditions in DMEM/F-12 medium (Gibco; Thermo Fisher Scientific, Waltham, Massachusetts,USA) supplemented with 10% fetal bovine serum (HyClone, GE Health Care; HyClone Laboratories Inc., Logan, USA), 1% antibiotic-antimycotic (Gibco). Cartilage harvesting was approved by the University of Berlin Ethics Committee (No. EA1/169_12), and the animal studies were approved by the Ethics Committee for animal experiments at Sahlgrenska University Hospital (Dnr 119–2015 and 36–2016).

2.3.3 Preparation of bioinks and 3D bioprinting (Study IV-V)

In study IV, processed adipose tissue was gently mixed with 3% (w/v) alginate Pronova SLG100 solution (Novamatrix, Sandvika, Norway) and 2.5% (w/v) tunicate nanocellulose dispersion (TuniCell ETC ; Ocean TuniCell AS, Bergen, Norway) in a ratio of 45:15:40 (tissue:alginate:nanocellulose). Blank samples (no fat tissue) were also prepared.

In study V, the hNCs were gently mixed with bioink consisting of an 80:20 mixture of tunicate nanocellulose (Ocean TuniCell, AS, Blomsterdalen, Norway) and alginate (SLG100; NovaMatrix, Sandvika, Norway). The hNC-to-ink ratio was 1:10, and the initial cell density was 10 x 10^6 cells/ml of bioink. Cell-free samples were also prepared.

Both fat- and chondrocyte containing constructs were 3D bioprinted (Inkredible+, CELLINK, Gothenburg, Sweden) as gridded square constructs (10 x 10 x 3 mm). An 18G conical nozzle was used, and the printing pressure was 11–13 kPa. The constructs were crosslinked with 100 mM $CaCl_2$ for 5 min, washed in culture medium (Dulbecco's modified Eagle medium/F-12; Life Technologies), and implanted shortly after printing.

2.3.4 Experimental animal model (Study IV-V)

The animal experiments were performed on 8-week old female BALB/c nude mice (Scanbur, Karlslunde, Denmark). For the implantation of the construct, as well as for the sequential MRI investigations the mice were anesthetized with isoflurane (Isoflurane Baxter, Baxter International).

In clean conditions, through a 10 mm dorsal incision, a subcutaneous pocket was created to fit the printed construct. The implants were inserted and the skin was sutured with 6/0 Vicryl Rapid (Ethicon, Bridgewater, New Jersey & Cincinnati, Ohio). No antibiotics were used. Body temperature was preserved with a heating pad placed under the animal.

During MRI the respiration was checked through a pressure sensitive pad (SA Instruments, Inc., NY, USA). A peripheral venous catheter was placed in the tail vein to infuse the Gadolinium based contrast agent. In both study IV and study V, the animals underwent MRI experiments with intravenous injection of contrast agent at up to 4 sequential timepoints after implantation. Following the final MRI, the animals were sacrificed and the 3D bioprinted construct explanted for analysis. Cell-free constructs were printed and treated in parallel in order to have material for comparison for histology as well as for in vivo MRI.

2.3.5 MRI techniques: DCE-MRI and DW-MRI (Study IV-V)

A preclinical, horizontal bore 7T MR system (Bruker BioSpin 70/20AS AVANCE I, GmbH, Germany; software: ParaVision 5.1) was used to collect MRI images (Fig.12). It was equipped with a maximum 400 mT/m gradient system and a 30-mm transmit/receive volume coil (RAPID Biomedical GmbH, Germany). Global 1st & 2nd order shimming was used to improve field homogeneity. Conventional 2-dimensional (2D) T2-weighted images covering the implant and surrounding anatomy were acquired in axial and coronal orientation using the rapid acquisition with relaxation enhancement (RARE) sequence with 1502 μm^2 in-plane resolution and 500 µm (axial) or 400 µm (coronal) slice thickness. An additional axial RARE scan with fat-suppression was acquired to visualize fat in, or surrounding, the implant. DWI was performed using a 2D single shot, spin-echo echo-planar imaging (SE-EPI) sequence, including 5 acquisitions without diffusion gradients (b=0 s/mm^2) and 12 acquisitions using b-values 50, 200, 400 and 900 s/mm^2 in 3 orthogonal diffusion directions. DCE images were acquired using the 2D retrospectively gated intra-gate fast low angle shot (IG-Flash) sequence, with 1500 repetitions during approximately 32 minutes for reconstruction of 32 time-frames. Navigator signal was derived from a 45 mm thick saturation slice including the image slices in parallel orientation. At the start of the acquisition of the 6th frame (5 min after the scan was started), the contrast agent solution (0.1 M Gd-DTPA, DOTAREM, Gothia Medical, Sweden, 0.3 mmol/kg bodyweight) was injected during ~10 sec. The total time for all MRI experiments was approximately 75 min per investigation.

Figure 12. The 7T small-animal MRI system

2.3.6 MRI studies postprocessing (Study IV-V)

The MRI data were processed with MATLAB (R2018b, The MathWorks, Inc., MA, USA). DCE-MRI signal intensity enhancement in the implant after contrast injection was analyzed voxel-wise as follows. The baseline voxel intensity was calculated as the mean signal intensity of the first five frames. The AT was defined as the time required from injection to the point at which signal intensity in a voxel was twice the voxel noise level above the baseline value. DCE functional color maps were generated by overlaying color-coded AT values from each 3D bioprinted construct to a baseline signal which corresponded to the signal in the surrounding tissue (mouse muscle tissue). Diffusion coefficient maps were calculated for each voxel by segmented bi-exponential model fitting only to b-values of 200, 400, and 900 s/mm^2. The median diffusion coefficient of each implant was calculated.

2.3.7 Histological and Immunohistochemical analysis (Study IV-V)

In both studies IV and V, after the final MRI, the constructs were harvested for histological and immunohistochemical analysis. The constructs were fixated in calcium-saturated 4% paraformaldehyde, dehydrated and embedded in paraffin. The constructs underwent horizontal sectioning discarding the superficial 1 mm and then saving the core sections, 5 µm thick. For histologic analysis the sections were stained with H&E in study IV and Alcian Blue, van Gieson and Saffranin-O in study V. For the immunohistochemical analysis slides were pretreated with citrate and immunostained with anti-CD31antibody (cat Nr ab134168, Abcam, dilution 1:150) (study IV and V) and anti-Ku80 antibody (cat Nr 2180, Cell Signaling Technology, dilution 1:800) (study IV).

2.3.8 Statistical analysis

The medians and interquartile ranges of the diffusion coefficients were calculated and graphed with SPSS (v22.0; IBM SPSS) and Microsoft Excel.

3. Results

3.1.1 Hb and HCT levels (Study I-II)

Study I

The mean HCT prior to hemodilution was 39.9 ± 0.01 % for the control group (group 1,) 38.9 ± 0.01 % for the ANH group (group 2), and 41.1 ± 0.07 % for AHH group (group 3), respectively. The mean HCT 24 h post-hemodilution was 36.2 ± 0.00 %, 26.8 ± 0.05 % and 28.1 ± 0.04 % ($p < 0.05$) for group 1, 2 and 3, respectively. Moreover, HCT was also assessed after 7 days in randomly selected animals in group 2 and 3 and the average postoperative HCT 7 days after the hemodilution was 27.6 %.

Study II

The mean HCT prior to hemodilution was 38.9 ± 0.04 % for group 1, 39.6 ± 0.02 % for group 2, and 38.9 ± 0.01 % for group 3, respectively. The mean HCT after the surgical procedure was 36.1 ± 0.00 %, 27.8 ± 0.04 % and 27.0 ± 0.03 % ($p < 0.05$ for group 2 and 3) for group 1, 2 and 3, respectively.

3.1.2 Direct observation (Study I-II)

Study I

The mean flap survival area was 70.6% ± 22.7 in group 1, 99.5 ± 0.93 in group 2, and 99.3 ± 1.30 in group 3, respectively. After 7 days the flap survival was higher in both hemodiluted groups (ANH and AHH) compared with the control ($p < 0.05$). When comparing flap survival between the ANH and AHH group, no significant differences were found ($p > 0.05$).

Study II

Overall, twisting the pedicle 90, 180, or 270 degrees had no effect on flap survival and no differences were found among the three main groups in terms of partial necrosis, change in skin color, edema or venous congestion. However, when a 360-degree torsion was applied ANOVA showed a higher flap survival rate ($p < 0.05$) in group 2 and 3 compared with group 1. However, this statistical significance did not persist after Bonferroni correction ($p = 0.07$ and $p = 0.09$ for group 2 and 3, respectively).

Detailed histological analysis of the animal in group 1-2-3 when 360° rotation was applied (subgroups IV) showed:

In group 1, subgroup IV, there were 1 total flap failure, 4 flaps with partial necrosis, 3 flaps with edema and venous congestion whereas 2 flaps survived without any complication.

In group 2, subgroup IV, there were 5 flaps with signs of venous congestion and edema while 5 flaps survived without any complication.

In group 3, subgroup IV, there were 6 flaps without any problems, 3 flaps with edema and signs of venous congestion and 1 flap had partial necrosis.

Overall, the mean flap survival rate was 81±18.4% in group 1, 100% survival in the group 2 and 98.7 ±2.4% in group 3, (Table 6).

360° Rotation	Total flap Necrosis	Partial flap necrosis	Edema / Congestion	No Complications	Mean flap survival %
CONTROL 10 flaps	**1 flap**	**4 flaps**	**3 flaps**	**2 flaps**	**81±18.3%**
% necrosis	**100%**	**8%;22%;26%;34%**			
ANH 10 flaps	**-**	**-**	**5 flaps**	**5 flaps**	**100%**
AHH 10 flaps	**-**	**1 flap**	**3 flaps**	**6 flaps**	**98.7 ±2.4%**
% necrosis		**13%**			

Table 6. Results obtained from the analysis of subgroup 4 (360° rotation).

3.1.3 Histological analysis (Study I-II)

Study I

In groups 1, 2 and 3, H&E staining of the tissue sections revealed signs of inflammation, edema, and congestion with a predominance of necrotic elements in group 1. Group 2 showed congestion but no signs of necrosis. In group 3 there was minor necrosis and edema signs.

Signs of thrombus formation in the anastomoses were present in all groups, with the exception of the arteries in ANH group.

In H&E staining, edema, congestion, inflammation necrosis, and thrombosis were graded using a semiquantitative scoring system: 0 = absence, 1 = mild, 2 = moderate, and 3 = severe.

Study II

In Subgroup IV (360º pedicle rotation), histopathologic examination of the SIEA flap showed signs of mild edema in group 1 and group 2 but severe edema and mild congestion in group 3. Necrosis was observed in groups 1 and 3 but not in group 2 (Table 7). In all groups, the section from the pedicle revealed signs of mild edema and moderate inflammation, but no signs of thrombosis were observed.

Subgroup 4 (360º pedicle rotation)	**Edema**	**Congestion**	**Inflammation**	**Necrosis**	**Thrombosis**
CONTROL flap	**1**	**0**	**2**	**0**	**0**
CONTROL pedicle	**1**	**0**	**3**	**1**	**0**
ANH flap	**1**	**1**	**2**	**0**	**0**
ANH pedicle	**1**	**0**	**2**	**0**	**0**
AHH flap	**1**	**1**	**2**	**1**	**0**
AHH pedicle	**3**	**1**	**2**	**1**	**0**

Table 7. Results obtained from the H&E staining analysis of subgroup 4, study II (360°Rotation).

3.1.4 Microangiography (Study I-II)

Study I and II

The images showed an improved blood supply in the flaps belong- ing to ANH and AHH groups in comparison with the control group supporting the direct observation. In study I, a larger vascularized area, was identified in group 2 (ANH group, 33.231 pixels); and in group 3 (AHH group, 1.612 pixels) compar ed with group 1 (Con-trol, 12.925 pixels).

Similarly, in study II, a larger vascularized area was identified in group 2 (ANH, 4.199 pixels) and 3 (AHH, 4.852 pixels) compared with group 1 (Control, 1.743 pixels) (Fig. 10).

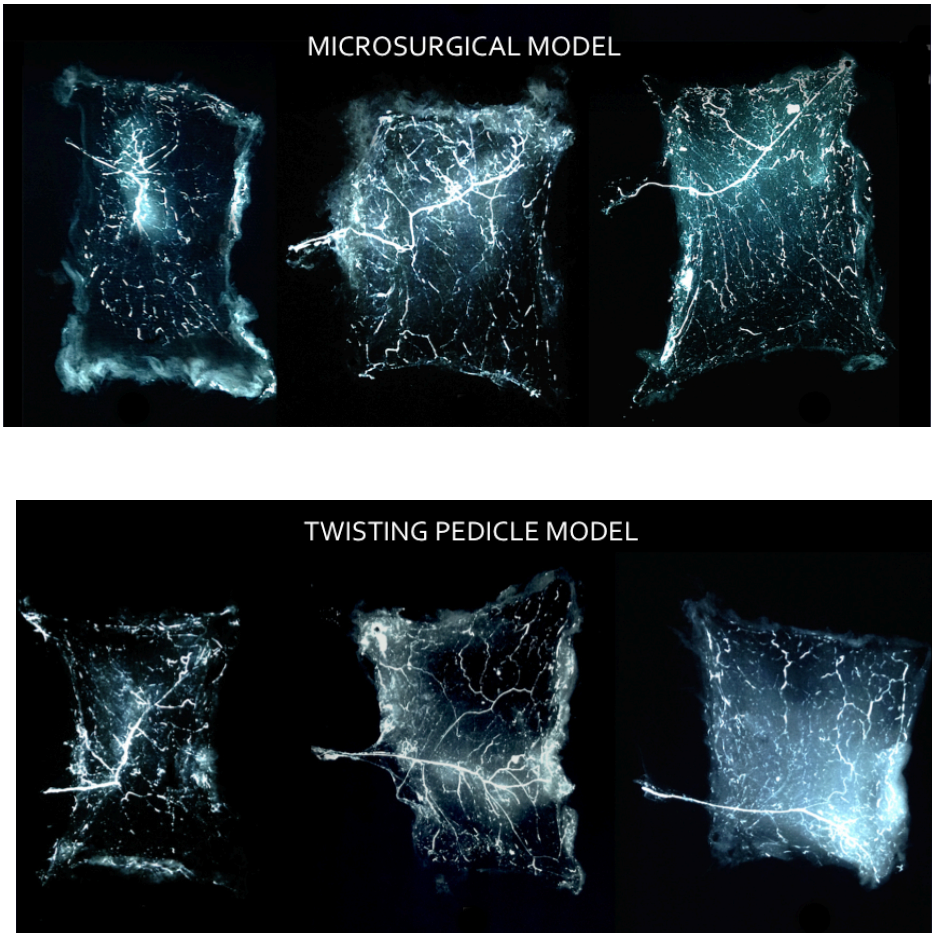

Figure 10. Microangiographic appearance of the flaps in study I(above) and II (below). Control flaps (left), ANH flaps (center), and AHH flaps (right). In both studies there were improved vascular patterns in both ANH and AHH groups.

3.2.1 Study selection and data extraction (Study III)

The systematic review was conducted according to the above-mentioned guidelines and included both clinical and experimental studies resulting in a total of 74 titles and abstracts. After exclusion of duplicates (n=5), 42 studies were also excluded since they did not match the predefined inclusion and exclusion criteria. The remaining studies were assessed by abstract review and 16 articles were found not relevant. Eleven full-text articles were retrieved and assessed for eligibility. Finally, only four studies fulfilled the criteria of our systematic review (Fig. 11). All included studies were experimental.

3.2.2 Risk of bias and quality assessment (Study III)

Assessment of the quality of evidence using the GRADE tool generated an overall low level of evidence in the 4 studies included. Several methodological weaknesses in study design and detection of uncertain aspects of bias using SYRCLE RoB tool, limited the quality of evidence. Moreover, risk-bias assessment across studies generated uncertain results (Table 8).

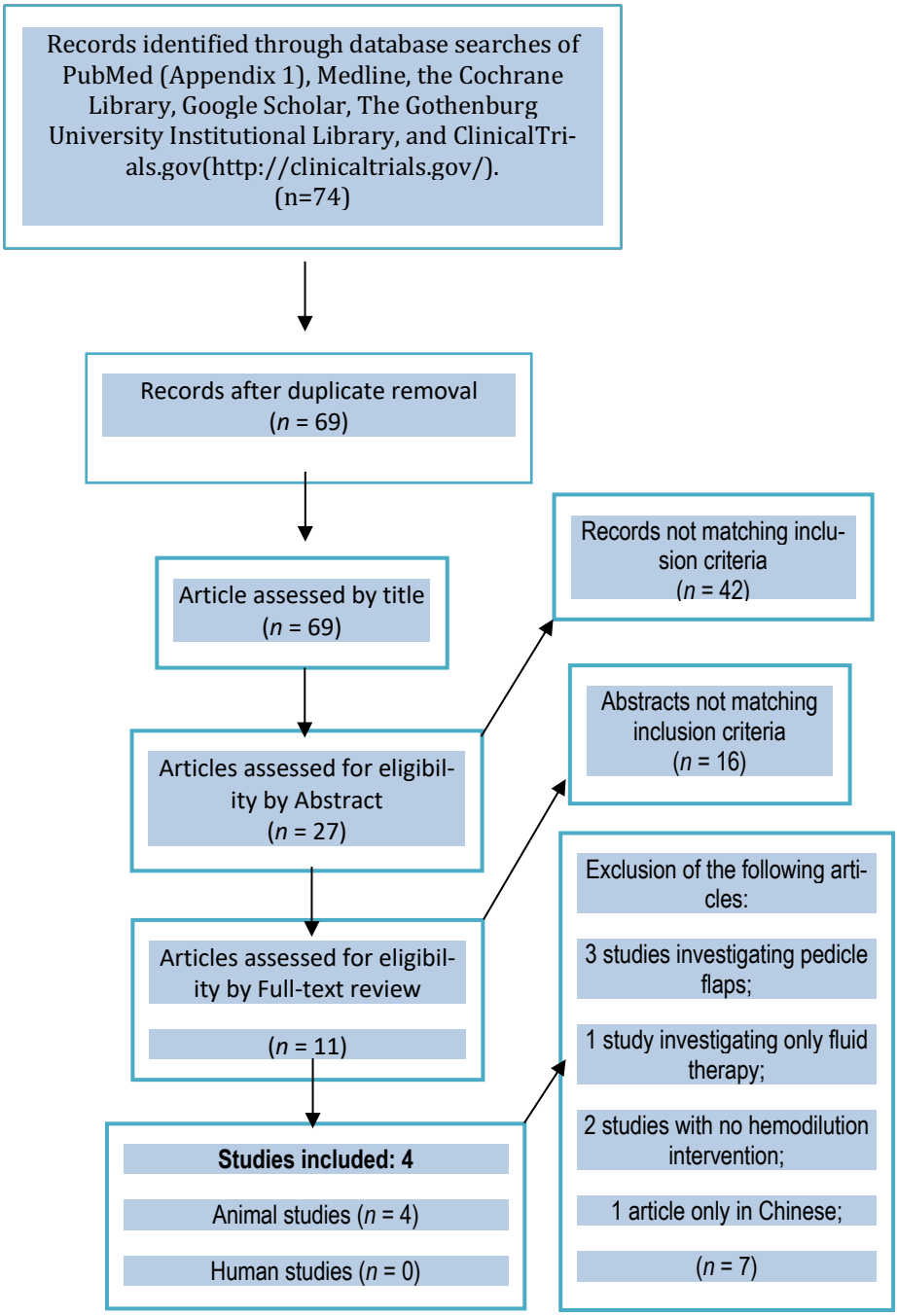

Figure 11. Flow chart of study selection.

Reference	Sample Size	Type of Surgery and Intervention	Time of Intervention	Comparator	Hemodilution protocol (ANH)	Fluid-replacement Protocol	Mean Htc value Pre- and Post-ANH (%)		Outcome	Quality of evidence (GRADE)
							Pre-ANH	Post-ANH		
Farina et al 2002	30	ANH in a thrombogenic model of SIEA flap	ANH preoperative	Control group (I) and a second experimental group (III)	(Gross formula)	The blood withdrawn was replaced with equivalent volume of 3% albumin	45.1	31.7	Significantly lower thrombosis rate of the microsurgical anastomosis in ANH group	Low
Farina et al 2006	40	ANH in a thrombogenic model of SIEA flap	ANH preoperative	Control group (I), administration of dextran-40 (group III), and administration of enoxaparin (group IV)	(Gross formula)	The blood withdrawn was replaced with equivalent volume of 3% albumin	46.2	30.7	Significantly lower thrombosis rate of the microsurgical anastomosis in ANH group	Low
Atchabahian et al 1996	50	ANH in a thrombogenic model of SIEA flap	ANH preoperative	Control group (I) and a second experimental group (II)	Withdrawal of 5–6 mL blood	Withdrawn blood was replaced with an equivalent volume of hydroxyethyl	N.R.	N.R.	Significantly lower thrombosis rate of the microsurgical anastomosis in ANH group	Low
Amoroso et al 2015	30	Microsurgical model of SIEA flap.	ANH 24-h before surgery	Control group (I) and a second experimental group (III)	(Gross formula)	Withdrawn blood was replaced with an equivalent volume of isotonic sodium chloride (0.9%) (two-thirds) plus hydroxyethyl starch (6%) (one-third)	38.9	26.8	Significantly lower rate of partial skin flap necrosis in ANH group	Low

SIEA, superficial inferior epigastric artery.

Table 8. Characteristics of the studies included according to the PICO criteria

3.3.1 MRI in vivo assessment of diffusion and perfusion (Study IV-V)

Study IV

Perfusion

Compared to the surrounding tissues, the bioprinted constructs had a long AT and low IS, indicating low perfusion in the constructs. The pattern remained unchanged during the study period.

Diffusion

The mean diffusion coefficient (D, $\mu m^2/ms$) was assessed in each of the 4 timepoints and it was relatively stable over the study period in both cell-containing or the cell-free constructs. The D values for each time point were 2.2 (1.9, 2.4) (median (25th and 75th percentiles)), 2.0 (1.7, 2.2), 2.0 (1.6, 2.4) and 2.0 (1.7, 2.4) while in the control group the pooled D was 2.58 (2.24, 2.89).

Study V

Perfusion

Initially the bioprinted constructs revealed longer AT and lower IS in all the printed constructs than in surrounding tissues. However, at the second/third timepoints, bioprinted constructs showed areas with shorter AT and higher IS (hot spots), corresponding to the location of the grid holes (Fig. 12). At 98 days, the overall perfusion patterns had a more homogenous distribution and hot spots were present in the bioprinted construct only in one animal. No hot spots, at any time-points, were found in constructs belonging to the control group.

Diffusion

The D was assessed at each timepoint showing a mean value of (all time points and voxels) 2.56 $\mu m^2/ms$ for the cell-containing constructs and 2.58 $\mu m^2/ms$ for the cell-free constructs. The median diffusion coefficient was similar and remained stable over time.

3.3.2 Histological and Immunohistochemical analysis (Study IV-V)

Study IV

Histologic examination of the 3D bioprinted fat constructs, explanted after the final MRI showed an abundance of preserved fat cells without signs of necrosis or inflammation. The grid structure could still be vaguely observed. Blood vessels both with and without erythrocytes could be seen. Immunohistochemical analysis confirmed CD 31-positive endothelial cells in vascular structures that were KU 80-positive in consecutive sections, pointing out the human origin of the vessel.

Study V

Macroscopic analysis of the 3D bioprinted constructs after explanation, revealed blood vessels on the surface of the constructs in both groups. The cell-containing constructs were well preserved, whereas some of the cell-free controls lost their shape and structure and were fragile.

Histological analysis of cell-containing constructs stained with H&E revealed preserved grid holes, with vascular structures containing erythrocytes. Alcian Blue van Gieson (ABvG) staining revealed chondrocyte clusters surrounded by glycosaminoglycans. Safranin-O staining confirmed production of proteoglycans in the extracellular matrix. No GAG- or proteoglycan-producing cells were

found in cell-free constructs. Immunohistochemical analysis showed CD 31-positive vascular structures both in the grid holes and on the surface of the constructs. The immunohistochemical analysis of collagen type II showed collagen in the same areas as the chondrocytes.

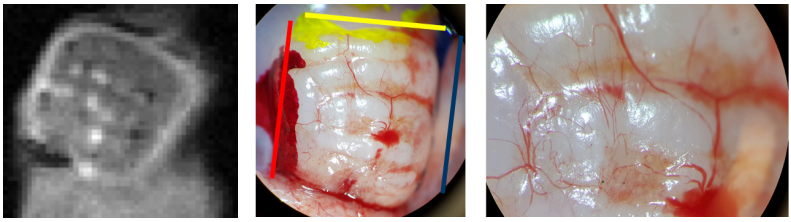

Figure 12. Dynamic contrast-enhanced MRI (DCE-MRI) image of the implanted construct obtained after intravenous administration of the contrast agent (Left). The white spots in the DCE-MRI image are areas of increased contrast signal intensity in the construct corresponding to the location of the grid holes (Middle and Right)

4. Discussion

4.1 Motivation and scope

Reconstructive microsurgery is a surgical technique used to transplant or replant tissues for reconstruction of defects or for restoration of function. Once the transplanted tissue is transferred into its recipient site, its viability is strictly related the re-establishment of an adequate blood flow in the flap. Inadequate vascularization will result in perfusion related complications (PRC). PRC are often multifactorial and result in flap ischemia as a result of thrombosis, hypoperfusion, and/or vasospasm at the microcirculation level. Besides the PRC risk, it is important to remember that any kind of free flap, per se, generate donor site morbidity. Therefore, tissue engineering techniques can be promising alternative sources of living tissue. 3D bioprinting is a future prospect for tissue regeneration due to the ability to create tissue-like constructs. Such constructs could be printed using the patients own cells and be used as biological substitutes. Lack of vascularization in the 3D bioprinted tissue represents one of the most critical challenges to overcome in order to advance this field toward its clinical application.

In the first part of this thesis, we aimed to provide solutions to the immediate problems related to PRC. This goal was achieved by studying the impact of hemodilution on microcirculation in free and pedicled flaps.

In the second part of this thesis, we aimed to study possibilities of vascularization of 3D bioprinted structures and thus, contribute to the development of a new technique that could reduce donor site morbidity.

4.2 Discussion of the main findings (Study I-II-III)

In order to reduce the rate of ischemic complications, it is necessary to guarantee an adequate blood perfusion in the flap.

This can be achieved, within certain limits by modifying the blood viscosity by reducing the HCT values, which determine about 98% of the viscosity of the blood. Several authors advocate normovolemic hemodilution as a tool able to increase both central and peripheral blood flow, without compromising tissue oxygenation [28, 31, 40, 41, 101].

During ANH, HCT is reduced as well as is the viscosity of the blood. This generates a reduction of the systemic vascular resistance with consequently improved venous return. All these mechanisms increase cardiac output (total flow rate) resulting in an increased in O_2 extraction, facilitating the O_2 transfer from the circulating blood to the tissue. ANH with HCT values around 30%, corresponding to hemoglobin (Hb) levels around 10 g/dl, is considered the optimal HCT value where the peach of O_2 extraction is reached [93, 102-104]. HCT values lower than 20% can compromise O_2 oxygenation in the tissues and therefore 20% HCT is considered the lower limit for a safe ANH [102, 104].

Studies have shown that the local tissue oxygenation is not reduced by ANH but instead become more homogeneous or slightly increased due to higher flux of red blood cell as a result of higher cardiac output [105].

Hemodilution can be obtained preoperatively by one or more autologous blood deposits [106] that are stored to be used perioperatively [84, 89, 107-109]. Preoperative autologous donation (PAD) of the patients own blood [106] is a frequently considered equivalent to acute normovolemic hemodilution. Because the donation of blood occurs in the weeks prior to operation, this time interval

allows for re-establishment of normal intravascular volume, without the need to infuse large volumes in conjunction with blood removal. Moreover, the blood units stored preoperatively, can be transfused to the patient if needed without exposing the patient to risk and sequel associated with adverse reaction to homologous transfusion [110].

ANH has been successfully used in several medical areas, such as cardiac surgery to reduce the high blood loss [111], neurosurgery for treatment of ischemic stroke, cardiovascular surgery [112], for treatment of central retinal vein thrombosis [113, 114], in orthopedic surgery [115, 116] or in elective surgery such as craniosynostosis operations [106]. Very little can be found in the literature on the effect of ANH and AHH when applied in reconstructive microsurgery.

Study I-II

Study I was designed to investigate the effect of ANH and AHH on flap survival in a microsurgical rat model. Concerning the first research question, whether hemodilution can improve the microcirculation through the changes in blood viscosity and reduce the incidence of partial necrosis of the flap, it was found that hemodilution treatment (ANH and AHH) applied 24 hours before surgery gave a beneficial effect on the viability of the free flap. However, there were no statistically significant differences between the 2 different hemodilution modalities in the study (ANH and AHH). One possible explanation for that could be related to the fact that ANH and AHH have similar effects on the rheological mechanisms in the populations studied. In rats, after a single acute blood draw of 1% of the animals body weight, it has been shown that it takes at least two weeks for the constituents of the blood to return to normal [117]. Therefore, it is likely that both ANH and AHH cause extended hemodilution, which could be seen as persistently reduced HCT also at day 7 in groups 2 and 3. However, this is the first study investigating the relationship between hemodilution and blood flow in a microsurgical free flap rat model.

Histopathological examination was undertaken to grade edema, congestion, inflammation necrosis, and thrombosis. The results showed a predominance of necrotic elements in the control group; minor necrosis and edema in the ANH group and congestion but no signs of necrosis in the AHH group. Microangiography showed that the blood supply in the periphery of the flaps in both hemodiluted groups (ANH and AHH) was improved. This finding broadly supports the observation of previous studies on hemodilution [28, 31, 40, 41, 101].

In study II, the research question focused on investigating the effect of ANH and AHH in a pedicled perforator flap with unfavorable hemodynamics. As in a propeller flap, various degrees of rotation were applied to the vascular pedicle, increasing the risk of hemodynamic complications. It is well known that pedicle twisting reduces arterial in-flow and venous out-flow. Moreover, it is known that due to the characteristics of the venous system, the veins are more sensitive to twisting, resulting in venous insufficiency and consequent flap congestion. However, this is the first study investigating the effects of pedicle torsion on flap viability during hemodilution in a rat model. Twisting the pedicle 90°, 180° and 270°, had no negative effect on flap survival. However, when 360° degrees of torsion (subgroup 4) was applied, both ANH and AHH resulted in higher (but not significantly higher survival, $p = 0.07$ and $p = 0.09$, respectively) compared to the control group. When comparing mean values of flap survival between the ANH and AHH, no significant differences were found.

It is somewhat surprising that no differences were noted between ANH and AHH, neither in study I, nor in study II. The reason for this is not clear but may be partly explained by physiologic compensatory mechanisms. Indeed, it could be hypothesized that physiologic diuresis re-establishes the initial intravascular volume by gradually reducing the 20% of additional liquids infused in the AHH group.

The hemodilution protocols used in these two first studies were slightly different as we adapted them to the two different surgical models. However, they both resulted in decreased blood viscosity by reducing HCT levels to values ranging from 27 to 30%. The degree of hemodilution chosen was based on the relationship existing between viscosity and hematocrit reported in the literature and HCT values of approximately 30 percent appears to optimal for the delicate balance between viscosity and oxygen-carrying capacity.

More than one formula has been proposed to calculate Total Blood Volume (TBV) in rats which is needed to calculate the blood volume to be withdrawn for hemodilution. In our pilot study we tested all of them and found the most trustworthy formula to be: 64ml per kg of body weight, i.e. for a 350g rat: 64 x 0,35 = 22.4 ml (Source: UK's National Centre for the Replacement, Refinement and Reduction of Animals in Research) [117]. Once the TBV is calculated, the Gross formula can be used to perform hemodilution treatment. The measured HCT values ended up very close to the predetermined ones. In AHH, the exact amount of isotonic fluid to infuse in order to achieve 20% volume expansion equals 20% of the estimated total blood volume. Irrespective of ANH or AHH, the hemodilution effectively maintained the reduction of post-hemodilution HCT values after 7 days. Microangiography revealed the flaps microvascular architecture and the improved vascular network in both hemodiluted groups compared with the control group in both studies I and II. Histopathologic examination with standard H&E staining of the SIEA flap showed inflammation, edema, and congestion in all groups with a predominance of necrotic elements in the control group.

We could say that both models support the proposed beneficial effect of hemodilution on microcirculation. The results obtained in study I and II may support the hypothesis that hemodilution improves blood perfusion and oxygenation in the flap, through reduction in blood viscosity. Moreover, both in study I and II the rheological benefit was confirmed by microangiography and histology. Prior

studies that have noted the clinical importance of ANH that has been used with success in various clinical areas. They have observed how the decrease in blood viscosity would generate an increase in blood flow due to the change in blood viscosity and through a reduction of the shear stress of red blood cells. Despite that, very little could be found in the literature on the relationship between hemodilution and flap survival in reconstructive microsurgery.

Study III

Study III aimed to establish the level of evidence for a beneficial effect of hemodilution on free flap microcirculation and flap survival in clinical and experimental settings. A systematic literature review was carried out with a defined search string and defined PICO criteria. A methodical analysis of the risk of bias and accurate assessment of the outcomes was carried out according to the SYRCLE's RoB and GRADE tools.

Initially, only clinical studies were considered, but due to the scarcity of studies retrieved during the search process, the research string was subsequently extended to include experimental studies as well.

Overall, the main evidence emerging from this systematic review is the scarcity of previous studies evaluating hemodilution applied in microsurgical reconstruction. Despite the clinical use of hemodilution in different surgical specialties, there is a lack of relevant clinical research. Moreover, the review revealed that hemodilution protocols are often largely based on personal assumptions rather than empiric evidence. Among the few clinical studies retrieved in our systematic review [108, 118-123] none of them satisfied the eligibility criteria of our systematic review and were therefore excluded.

In contrast to clinical studies, we found experimental animal models reporting positive effects of hemodilution. The preclinical studies included in this review (n = 4)[124-127] investigated the effect of hemodilution using different microsurgical models *in vivo*.

The reduced HCT value (27% - 30%) was effective in improving flap perfusion and flap survival rate [124-127]. Among the 4 studies, 3 focused on the protective effect of hemodilution on the thrombosis rate at the level of the anastomosis rather than flap perfusion [125-127]. Studies on hemodilution and microcirculation in free flaps are limited to that of Amoroso et al. [124].

Future research in this field needs to be designed to raise the level of evidence. Differences between rats and humans in terms of coagulation properties and response to hemodilution need to be considered. The use of a hemodilution protocol and strict inclusion criteria is needed. In terms of study design, future studies should be prospective, randomized and correctly powered. Anti-thrombotic treatment is another major topic in microsurgery that might interfere with hemodilution effects and its exclusion or exclusion from the clinical trial might significatively interfere with the results.

4.3. Discussion of the main findings (study IV-V)

3D bioprinting techniques have the potential to address the problem of limited source of tissue for reconstructive surgery. At the same time, 3D bioprinting would address the problems with donor site morbidity. One main obstacle in 3D bioprinting research is the lack of vascularization [84, 89, 108]. Indeed, supply of oxygen and nutrients to the construct is often restricted to diffusion that can only supply cells in a proximity of 100–200 mm. Therefore, constructs depending totally on diffusion could not be thicker than 0.5 mm. If lager implanted constructs should survive, they need vascularization. Spontaneous vascular ingrowth is slow [128]. In order to improve the speed of vascularization after implantation different strategies have been proposed. A central factor of blood-vessel formation is strictly related to presence, and size of pores within the construct. Druecke et al. demonstrated that vessel growth in scaffolds with pores

greater than 250 mm was significantly faster than in those with smaller pores [129].

Moreover, the interconnectivity of the pores influence cell migration. Customizable 3D bioprinted scaffolds loaded with cells can be created with interconnected pores in order to facilitate vascularization. Our research group previously presented a method for 3D bioprinting of human adipose tissue constructs with dimensions much larger than the diffusion range of oxygen using human lipoaspirate-derived adipose tissue (LAT). The constructs were able to survive *in vivo* and contained functioning blood vessels self-generated by either by spontaneous ingrowth of vascular structures from the host or from the fragments of blood vessels present in the LAT [130].

Study IV

Study IV aimed to investigate vascularization of 3D bioprinted LAT constructs. We studied perfusion and diffusion properties in the constructs, *in vivo*, over a period of 99 days using MRI. The constructs were also histologically and immunohistochemically examined. The size of the bioprinted constructs were 10 x 10 x 3 mm, i.e., considerably larger than what can be expected to survive by diffusion only.

After 3 months of *in vivo* implantation, the bioprinted constructs survived in their whole, showing well-preserved adipose tissue with no signs of necrosis or inflammation at the histopathological analysis. The most interesting finding was the presence of a vascular network in the bioprinted constructs. Some of these vessels were of human origin and they contained erythrocytes, i.e., they were interconnected with the circulation of the host. Taken together, this study showed spontaneous vascularization of 3D bioprinted LAT. The DWI- MRI finding of long AT value and the low IS indicated that perfusion in the constructs was lower than in the surrounding tissue pointing at diffusion as the predominant mechanism responsible for the transport of oxygen and nutrients. However, the

diffusion coefficient (D) was relatively high and constant over time. That could well be an important finding pointing at favorable characteristics of the biomaterial. The nanocellulose bioink used has a very high water content and printing with such ink allows both spatial distribution of the cells and tissues included and at the same time favorable diffusion that contributes to cell survival.

Study V

In Study V, we aimed to investigate changes in perfusion and diffusion properties in 3D bioprinted human cartilage constructs, *in vivo*, over a 98 days period. The same methodology and study design used in study IV was used in study V. After 3 months of in vivo implantation the bioprinted constructs survived in their whole, showing well-preserved chondrocytes with no signs of necrosis or inflammation. The D was relatively stable over time in both chondrocyte laden constructs and in the cell-free control group. As in study 4, this could reflect the favorable characteristics of the biomaterial used. On day 0, a longer AT and a lower IS signal was seen in the printed constructs compared to the surrounding tissues. At day 30, we observed areas having shorter AT and higher IS, hot spots corresponding to the grid holes. Signal intensity in the hot spots after contrast administration was similar to that of the aorta suggesting a connection with the host vasculature. This finding was observed on the majority of the 3D bioprinted chondrocyte constructs, but not in the control group. The chondrocyte proliferation was assessed histologically and immunohistochemically by the presence of proliferation in clusters and by their production of GAG and collagen type II. A distance between the chondrocytes and the grid holes was observed. This could indicate that these cells prefer a particular oxygen pressure.

In summary, the grid structure promoted in-growth of blood vessels from the host.

5. Conclusions

The principal conclusions are:

Study I

Both normovolemic and hypervolemic hemodilution was effective in improving the microcirculation in a free flap rat model.

Study II

Both normovolemic and hypervolemic hemodilution was effective in improving the microcirculation in a pedicled twisted flap rat model.

Study III

There is a lack of relevant evidence supporting the positive effect of hemodilution on microcirculation in free flaps in both clinical and experimental studies.

Study IV

3D bioprinting with LAT allows spontaneous vascularization of the bioprinted constructs.

Study V

A gridded structure of 3D bioprinted cartilage promote in-growth of blood vessels

6. Future Perspectives

The results obtained in study I and II support the hypothesis that hemodilution could reduce the risk of PRC. On the other hand, due to the lack of clinical relevance existing in the medical literature on this topic, as shown by the systematic literature analysis in study III, the beneficial effect of hemodilution on microcirculation in free flaps needs further investigation. Therefore, a large randomized prospective clinical study on hemodilution, using a rigorous protocol, strict inclusion criteria to select patients and randomly allocate them in 2 groups of study (hemodilution vs control), would be needed to validate the potential benefit of hemodilution in reconstructive microsurgery.

The experimental studies IV and V show two different ways to achieve vascularization in 3D bioprinted tissue; spontaneous formation of blood vessels from the tissue included in the bioprinting process and ingrowth of blood vessels from the host, facilitated by a gridded structure.

The next step would be to print larger constructs to challenge the limits of this technique. Also, a switch to an immune-competent model is necessary and further experiments are needed before transition to the clinic.

7. Acknowledgements

An aspect that played a central role in the realization of the studies included in this doctoral thesis has been the effective scientific collaborations established between my current institution, the Department of Plastic Surgery, Institute of Clinical Sciences, Sahlgrenska Academy, University of Gothenburg, the Department of Plastic Surgery, Akdeniz University Hospital, Antalya, Turkey, the 3D Bioprinting Center, BBV at Biotech Center, Department of Chemistry and Chemical Engineering, Chalmers University of Technology and the Department of Radiology, Sahlgrenska Academy, University of Gothenburg.

I would like to express my sincere gratitude to **the University of Gothenburg, Sahlgrenska Academy**; represented by **Peter Naredi,** Head of the Institute of Clinical Sciences, all the **co-authors** that contributed to the realization of the studies included in this PhD thesis and have supported my professional achievement during these past 5 years.

In particular, I would like to thank:

Professor Lars Kölby, my principal supervisor, for the time and energy spent correcting and improving this thesis, thanks for your support, constructive feedback, positive attitude, and enthusiasm for sharing knowledge and ideas with me. Thanks for your positive attitude and humor. Last but not least, thanks for all your precious advice along the way.

Karin Säljö, assistant supervisor and co-author, for her contribution in reviewing processing this thesis with valuable feedback and scientific discussion. Thank your professional assistance and active collaboration in the research team.

Professor Anna Elander, my chief and current head of the Department of Plastic Surgery, Sahlgrenska University Hospital, for believing in me and supporting me since I first moved to Göteborg in 2015.

Peter Apelgren, Section head of the Department of Plastic Surgery, Sahlgrenska University Hospital, for his participation as co-author, for his remarkable contribution and good teamwork in all the experiments involving the 3D bioprinting. For his active collaborations, including writing process of research papers and daily clinical work.

Professor Paul Gatenholm, Director of 3D Bioprinting Center, at Biotech Center, Chalmers University of Technology, Göteborg, for making our scientific collaboration possible and for having being been able to bring together our different disciplines in a fruitful way toward a common goal.

Michael Montelius. for the important contribution as co-author and for sharing his knowledge and expertise in the field of magnetic resonance imaging. Thanks for your central contribution in planning and carrying out the MRI studies and with the manuscript always taking the time to explain and discuss the experimental methods and results.

Mona Engström, for the precious help you provided carrying out the immuno-histochemical analysis in study IV and V.

Hector Martinez Avila and Linnea Strid Orrhult, from the 3D bioprinting cen-ter at Chalmers, University of Technology, for their significant contribution with the parts of the projects related to the 3D bioprinting process.

Professor Ömer Özkan, head of the Department of Plastic Surgery at the Ak-deniz University Hospital, Antalya, Turkey, for making our scientific collabora-tions possible, for his giving me his trust and availability during these past years.

Özlenen Özkan, for her contribution with the studies I and II and for her support and hospitality during my stay at the plastic surgery department in Antalya.

Professor Hung Chi Chen, head of the Department of Plastic Surgery, China Medical University Hospital, for the extensive clinical training provided to me during the 1-year fellowship program in Advanced Reconstructive Microsurgery in Taiwan. I will always be grateful to you for making me a better surgeon and for being a model of personal humility and professional excellence.

Professor Joon Pio Hong, head of the Plastic Surgery Department at Asan Medical Center, Seoul, South Korea for sharing your deep knowledge, valuable advices and good friendship.

Erol Nizamoglu for his expertise in experimental microsurgery and his important contribution with the experiments carried out in study I and II. I will be always grateful for your true friendship.

All my colleagues at the plastic surgery department for their support during the time I have been working on my project. Thank you guys!

Madiha Bhatti Söfteland, for being a good colleague and sincere friend for many years.

Giovanni Maltese and Gennaro Selvaggi for your support and experience as colleagues but above all for being good friends i can rely on and trust.

Onur Ogan and Kerim Ünal for their sincere friendship and for the wonderful memories together.

Federico, my little brother, for his constant encouragement and for always being each other´s rocks. ¨

Alessandro, the closest thing to a brother I would say. Thanks for always being present in my life and for your true friendship for the past 22 years.

Last but not least, I would like to thank **my wonderful parents**.
When I left my country to follow my ambitions many years ago, they knew that this meant that their “child” wouldn’t be able to be back home so often. Despite that, they have always been encouraging and supporting in my everyday life. Their dedication to the family and their love, allowed me to live a privileged life and to follow my passions without fear.
I believe my success is their success and this book just prove that.

8. References

1. Tagliacozzi, G., *De curtorum chirurgia per insitionem,*. 1597.

2. Al-Himdani, S., et al., *Tissue-Engineered Solutions in Plastic and Reconstructive Surgery: Principles and Practice.* Front Surg, 2017. **4**: p. 4.

3. Krizek, T.J., et al., *Experimental transplantation of composite grafts by microsurgical vascular anastomoses.* Plast Reconstr Surg, 1965. **36**(5): p. 538-46.

4. McLean, D.H. and H.J. Buncke, Jr., *Autotransplant of omentum to a large scalp defect, with microsurgical revascularization.* Plast Reconstr Surg, 1972. **49**(3): p. 268-74.

5. Daniel, R.K. and G.I. Taylor, *Distant transfer of an island flap by microvascular anastomoses. A clinical technique.* Plast Reconstr Surg, 1973. **52**(2): p. 111-7.

6. Song, R., et al., *The forearm flap.* Clin Plast Surg, 1982. **9**(1): p. 21-6.

7. Taylor, G.I. and J.H. Palmer, *The vascular territories (angiosomes) of the body: experimental study and clinical applications.* Br J Plast Surg, 1987. **40**(2): p. 113-41.

8. Koshima, I. and S. Soeda, *Inferior epigastric artery skin flaps without rectus abdominis muscle.* Br J Plast Surg, 1989. **42**(6): p. 645-8.

9. Song, Y.G., G.Z. Chen, and Y.L. Song, *The free thigh flap: a new free flap concept based on the septocutaneous artery.* Br J Plast Surg, 1984. **37**(2): p. 149-59.

10. Holmström, H., *The free abdominoplasty flap and its use in breast reconstruction. An experimental study and clinical case report.* Scand J Plast Reconstr Surg, 1979. **13**(3): p. 423-27.

11. Munder, B., et al., *The DIEP Flap as Well-established Method of Choice for Autologous Breast Reconstruction with a Low Complication Rate - Retrospective Single-centre 10-Year Experience.* Geburtshilfe Frauenheilkd, 2020. **80**(6): p. 628-638.

12. Pribaz, J.J. and N.A. Fine, *Prelamination: defining the prefabricated flap--a case report and review.* Microsurgery, 1994. **15**(9): p. 618-23.

13. Yao, S.T., *Microvascular transplantation of prefabricated free thigh flap.* Plast Reconstr Surg, 1982. **69**(3): p. 568.

14. Ozkan, O., I. Koshima, and K. Gonda, *A supermicrosurgical flap model in the rat: a free true abdominal perforator flap with a short pedicle.* Plast Reconstr Surg, 2006. **117**(2): p. 479-85.

15. Wei, F.C., et al., *Confusion among perforator flaps: what is a true perforator flap?* Plast Reconstr Surg, 2001. **107**(3): p. 874-6.

16. Tamai, S., *History of microsurgery--from the beginning until the end of the 1970s.* Microsurgery, 1993. **14**(1): p. 6-13.

17. Chana, J.S. and F.C. Wei, *A review of the advantages of the anterolateral thigh flap in head and neck reconstruction.* Br J Plast Surg, 2004. **57**(7): p. 603-9.

18. May, J.W., Jr., G.G. Gallico, 3rd, and F.N. Lukash, *Microvascular transfer of free tissue for closure of bone wounds of the distal lower extremity.* N Engl J Med, 1982. **306**(5): p. 253-7.

19. Suh, J.D., et al., *Analysis of outcome and complications in 400 cases of microvascular head and neck reconstruction.* Arch Otolaryngol Head Neck Surg, 2004. **130**(8): p. 962-6.

20. Laurie, S.W., et al., *Donor-site morbidity after harvesting rib and iliac bone.* Plast Reconstr Surg, 1984. **73**(6): p. 933-8.

21. Hallock, G.G., *Relative donor-site morbidity of muscle and fascial flaps.* Plast Reconstr Surg, 1993. **92**(1): p. 70-6.

22. Blondeel, N., et al., *The donor site morbidity of free DIEP flaps and free TRAM flaps for breast reconstruction.* Br J Plast Surg, 1997. **50**(5): p. 322-30.

23. Colen, S.R., W.W. Shaw, and J.G. McCarthy, *Review of the morbidity of 300 free-flap donor sites.* Plast Reconstr Surg, 1986. **77**(6): p. 948-53.

24. Suominen, S., J. Ahovuo, and S. Asko-Seljavaara, *Donor site morbidity of radial forearm flaps. A clinical and ultrasonographic evaluation.* Scand J Plast Reconstr Surg Hand Surg, 1996. **30**(1): p. 57-61.

25. Richardson, D., et al., *Radial forearm flap donor-site complications and morbidity: a prospective study.* Plast Reconstr Surg, 1997. **99**(1): p. 109-15.

26. Jones, M.Z.G., *Reconstructive Surgery: Anatomy, Technique, and Clinical Application*. 2012: Thieme Publishers,. 1849.

27. Sasmor, M.T., et al., *Vascular resistance considerations in free-tissue transfer.* J Reconstr Microsurg, 1992. **8**(3): p. 195-200.

28. Hagau, N. and D. Longrois, *Anesthesia for free vascularized tissue transfer.* Microsurgery, 2009. **29**(2): p. 161-7.

29. Fåhræus, R. and T. Lindqvist, *The viscosity of the blood in narrow capillary tubes.* Am J Physiol 1931. **96**(3): p. 562–568,.

30. Guyton, A.C., et al., *Blood pressure regulation: basic concepts.* Fed Proc, 1981. **40**(8): p. 2252-6.

31. Macdonald, D.J., *Anaesthesia for microvascular surgery. A physiological approach.* Br J Anaesth, 1985. **57**(9): p. 904-12.

32. Chen, L.E., et al., *The effect of acute denervation on the microcirculation of skeletal muscle: rat cremaster model.* J Orthop Res, 1991. **9**(2): p. 266-74.

33. Siemionow, M., et al., *Effect of muscle flap denervation on flow hemodynamics: a new model for chronic in vivo studies.* Microsurgery, 1994. **15**(12): p. 891-4.

34. Wang, W.Z., G. Anderson, and J.C. Firrell, *Arteriole constriction following ischemia in denervated skeletal muscle.* J Reconstr Microsurg, 1995. **11**(2): p. 99-106.

35. Vedder NB, *Flap physiology*, in *General Principles- Plastic Surgery* , Mathes SJ, Editor. 2005, Saunders 2005. p. pp 486–488.

36. Motakef, S., et al., *Emerging paradigms in perioperative management for microsurgical free tissue transfer: review of the literature and evidence-based guidelines.* Plast Reconstr Surg, 2015. **135**(1): p. 290-9.

37. Karladani, A.H., et al., *Salvaged limbs after tibial shaft fractures with extensive soft-tissue injury: a biopsychosocial function analysis.* J Trauma, 2001. **50**(1): p. 60-4.

38. Rosberg, B. and K. Wulff, *Regional blood flow in normovolaemic and hypovolaemic haemodilution. An experimental study.* Br J Anaesth, 1979. **51**(5): p. 423-30.

39. Gatti, J.E., et al., *Altered skin flap survival and fluorescein kinetics with hemodilution.* Surgery, 1982. **92**(2): p. 200-5.

40. Sigurdsson, G.H., *Perioperative fluid management in microvascular surgery.* J Reconstr Microsurg, 1995. **11**(1): p. 57-65.

41. Schramm, S., et al., *Acute normovolemic hemodilution improves oxygenation in ischemic flap tissue.* Anesthesiology, 2002. **96**(6): p. 1478-84.

42. Earle, A.S., R.B. Fratianne, and F.D. Nunez, *The relationship of hematocrit levels to skin flap survival in the dog.* Plast Reconstr Surg, 1974. **54**(3): p. 341-44.

43. Oppitz, P.P. and M.A. Stefani, *Acute normovolemic hemodilution is safe in neurosurgery.* World Neurosurg, 2013. **79**(5-6): p. 719-24.

44. Kuo, L. and R.N. Pittman, *Effect of hemodilution on oxygen transport in arteriolar networks of hamster striated muscle.* Am J Physiol, 1988. **254**(2 Pt 2): p. H331-9.

45. Mirhashemi, S., et al., *Microcirculatory effects of normovolemic hemodilution in skeletal muscle.* Int J Microcirc Clin Exp, 1987. **6**(4): p. 359-69.

46. Messmer, K., et al., *Acute normovolemic hemodilution. Changes of central hemodynamics and microcirculatory flow in skeletal muscle.* Eur Surg Res, 1972. **4**(1): p. 55-70.

47. Groll, J., et al., *Biofabrication: reappraising the definition of an evolving field.* Biofabrication, 2016. **8**(1): p. 013001.

48. Murphy, S.V. and A. Atala, *3D bioprinting of tissues and organs.* Nat Biotechnol, 2014. **32**(8): p. 773-85.

49. Cui, X., et al., *Thermal inkjet printing in tissue engineering and regenerative medicine.* Recent Pat Drug Deliv Formul, 2012. **6**(2): p. 149-55.

50. Mandrycky, C., et al., *3D bioprinting for engineering complex tissues.* Biotechnol Adv, 2016. **34**(4): p. 422-434.

51. Cui, X., et al., *Cell damage evaluation of thermal inkjet printed Chinese hamster ovary cells.* Biotechnol Bioeng, 2010. **106**(6): p. 963-9.

52. Peltola, S.M., et al., *A review of rapid prototyping techniques for tissue engineering purposes.* Ann Med, 2008. **40**(4): p. 268-80.

53. Gruene, M., et al., *Laser printing of stem cells for biofabrication of scaffold-free autologous grafts.* Tissue Eng Part C Methods, 2011. **17**(1): p. 79-87.

54. Guillotin, B. and F. Guillemot, *Cell patterning technologies for organotypic tissue fabrication.* Trends Biotechnol, 2011. **29**(4): p. 183-90.

55. Koch, L., et al., *Laser printing of skin cells and human stem cells.* Tissue Eng Part C Methods, 2010. **16**(5): p. 847-54.

56. Williams D.F., *On the nature of biomaterials.* Biomaterials, 2009. **30**: p. 5897- 909.

57. Frampton, J.P., et al., *Fabrication and optimization of alginate hydrogel constructs for use in 3D neural cell culture.* Biomed Mater, 2011. **6**(1): p. 015002.

58. Khalil, S. and W. Sun, *Bioprinting endothelial cells with alginate for 3D tissue constructs.* J Biomech Eng, 2009. **131**(11): p. 111002.

59. Almeida, C.R., et al., *Impact of 3-D printed PLA- and chitosan-based scaffolds on human monocyte/macrophage responses: unraveling the effect of 3-D structures on inflammation.* Acta Biomater, 2014. **10**(2): p. 613-22.

60. Song, S.J., et al., *A three-dimensional bioprinting system for use with a hydrogel-based biomaterial and printing parameter characterization.* Artif Organs, 2010. **34**(11): p. 1044-8.

61. Lee, V., et al., *Design and fabrication of human skin by three-dimensional bioprinting.* Tissue Eng Part C Methods, 2014. **20**(6): p. 473-84.

62. Möller, T., et al., *In Vivo Chondrogenesis in 3D Bioprinted Human Cell-laden Hydrogel Constructs.* Plast Reconstr Surg Glob Open, 2017. **5**(2): p. e1227.

63. Coleman, W.P., 3rd, *The history of liposuction and fat transplantation in America.* Dermatol Clin, 1999. **17**(4): p. 723-7, v.

64. Toledo, L.S. and R. Mauad, *Fat injection: a 20-year revision.* Clin Plast Surg, 2006. **33**(1): p. 47-53, vi.

65. Rigotti, G., et al., *Clinical treatment of radiotherapy tissue damage by lipoaspirate transplant: a healing process mediated by adipose-derived adult stem cells.* Plast Reconstr Surg, 2007. **119**(5): p. 1409-1422.

66. Hallock, G.G., *Complications of the free-flap donor site from a community hospital perspective.* J Reconstr Microsurg, 1991. **7**(4): p. 331-4.

67. Luquetti, D.V., E. Leoncini, and P. Mastroiacovo, *Microtia-anotia: a global review of prevalence rates.* Birth Defects Res A Clin Mol Teratol, 2011. **91**(9): p. 813-22.

68. Tanzer, R.C., *Total reconstruction of the external ear.* Plast Reconstr Surg Transplant Bull, 1959. **23**(1): p. 1-15.

69. Firmin, F. and A. Marchac, *[Reconstruction of the burned ear].* Ann Chir Plast Esthet, 2011. **56**(5): p. 408-16.

70. Osorno, G., *Autogenous rib cartilage reconstruction of congenital ear defects: report of 110 cases with Brent's technique.* Plast Reconstr Surg, 1999. **104**(7): p. 1951-62; discussion 1963-4.

71. Nava, M.M., et al., *The effect of scaffold pore size in cartilage tissue engineering.* J Appl Biomater Funct Mater, 2016. **14**(3): p. e223-9.

72. Maidhof, R., et al., *Biomimetic perfusion and electrical stimulation applied in concert improved the assembly of engineered cardiac tissue.* J Tissue Eng Regen Med, 2012. **6**(10): p. e12-23.

73. Yue, Z., et al., *Preparation of three-dimensional interconnected macroporous cellulosic hydrogels for soft tissue engineering.* Biomaterials, 2010. **31**(32): p. 8141-52.

74. Hollister, S.J., *Porous scaffold design for tissue engineering.* Nat Mater, 2005. **4**(7): p. 518-24.

75. Den Buijs, J.O., D. Dragomir-Daescu, and E.L. Ritman, *Cyclic deformation-induced solute transport in tissue scaffolds with computer designed, interconnected, pore networks: experiments and simulations.* Ann Biomed Eng, 2009. **37**(8): p. 1601-12.

76. Den Buijs, J.O., et al., *Solute transport in cyclically deformed porous tissue scaffolds with controlled pore cross-sectional geometries.* Tissue Eng Part A, 2009. **15**(8): p. 1989-99.

77. Carrier, R.L., et al., *Perfusion improves tissue architecture of engineered cardiac muscle.* Tissue Eng, 2002. **8**(2): p. 175-88.

78. Sooppan, R., et al., *In Vivo Anastomosis and Perfusion of a Three-Dimensionally-Printed Construct Containing Microchannel Networks.* Tissue Eng Part C Methods, 2016. **22**(1): p. 1-7.

79. Burghartz, M., et al., *Vascularization of engineered cartilage constructs in a mouse model.* Cell Tissue Res, 2015. **359**(2): p. 479-487.

80. Radisic, M., et al., *Oxygen gradients correlate with cell density and cell viability in engineered cardiac tissue.* Biotechnol Bioeng, 2006. **93**(2): p. 332-43.

81. Bertassoni, L.E., et al., *Hydrogel bioprinted microchannel networks for vascularization of tissue engineering constructs.* Lab Chip, 2014. **14**(13): p. 2202-11.

82. Flamme, I. and W. Risau, *Induction of vasculogenesis and hematopoiesis in vitro.* Development, 1992. **116**(2): p. 435-9.

83. Tomasina, C., et al., *Bioprinting Vasculature: Materials, Cells and Emergent Techniques.* Materials (Basel), 2019. **12**(17).

84. Auger, F.A., L. Gibot, and D. Lacroix, *The pivotal role of vascularization in tissue engineering.* Annu Rev Biomed Eng, 2013. **15**: p. 177-200.

85. Richards, D., et al., *3D Bioprinting for Vascularized Tissue Fabrication.* Ann Biomed Eng, 2017. **45**(1): p. 132-147.

86. Laschke, M.W., et al., *Angiogenesis in tissue engineering: breathing life into constructed tissue substitutes.* Tissue Eng, 2006. **12**(8): p. 2093-104.

87. Lokmic, Z. and G.M. Mitchell, *Engineering the microcirculation.* Tissue Eng Part B Rev, 2008. **14**(1): p. 87-103.

88. Rouwkema, J., N.C. Rivron, and C.A. van Blitterswijk, *Vascularization in tissue engineering.* Trends Biotechnol, 2008. **26**(8): p. 434-41.

89. Sarker, M.D., et al., *3D biofabrication of vascular networks for tissue regeneration: A report on recent advances.* J Pharm Anal, 2018. **8**(5): p. 277-296.

90. Zhang, H.B., et al., *Three-dimensional bioprinting is not only about cell-laden structures.* Chin J Traumatol, 2016. **19**(4): p. 187-92.

91. Kang, H.W., et al., *A 3D bioprinting system to produce human-scale tissue constructs with structural integrity.* Nat Biotechnol, 2016. **34**(3): p. 312-9.

92. Xie, C., et al., *Structure-induced cell growth by 3D printing of heterogeneous scaffolds with ultrafine fibers.* Materials & Design, 2019. **181**(05 November).

93. Sanders, J.E., A.B. Baker, and S.L. Golledge, *Control of in vivo microvessel ingrowth by modulation of biomaterial local architecture and chemistry.* J Biomed Mater Res, 2002. **60**(1): p. 36-43.

94. Zheng, Y., et al., *Microstructured templates for directed growth and vascularization of soft tissue in vivo.* Biomaterials, 2011. **32**(23): p. 5391-401.

95. Raya, J.G., *Techniques and applications of in vivo diffusion imaging of articular cartilage.* J Magn Reson Imaging, 2015. **41**(6): p. 1487-504.

96. Moher, D., et al., *PRISMA statement.* Epidemiology, 2011. **22**(1): p. 128; author reply 128.

97. Turner, R.M., S.M. Bird, and J.P. Higgins, *The impact of study size on meta-analyses: examination of underpowered studies in Cochrane reviews.* PLoS One, 2013. **8**(3): p. e59202.

98. Mettes, T.G., et al., *Impact of guideline implementation on patient care: a cluster RCT.* J Dent Res, 2010. **89**(1): p. 71-6.

99. Hooijmans, C.R., et al., *SYRCLE's risk of bias tool for animal studies.* BMC Med Res Methodol, 2014. **14**: p. 43.

100. Guyatt, G., et al., *A guide to GRADE guidelines for the readers of JTH.* J Thromb Haemost, 2013. **11**(8): p. 1603-8.

101. Hanasono, M.M., et al., *Changes in blood velocity following microvascular free tissue transfer.* J Reconstr Microsurg, 2009. **25**(7): p. 417-24.

102. Clark, J.R., et al., *Predictors of morbidity following free flap reconstruction for cancer of the head and neck.* Head Neck, 2007. **29**(12): p. 1090-101.

103. Hint, H., *The pharmacology of dextran and the physiological background for the clinical use of rheomacrodex and macrodex.* Acta Anaesthesiol Belg, 1968. **19**(2): p. 119-38.

104. Murray, D., *Acute normovolemic hemodilution.* Eur Spine J, 2004. **13 Suppl 1**: p. S72-5.

105. Kreimeier, U. and K. Messmer, *Perioperative hemodilution.* Transfus Apher Sci, 2002. **27**(1): p. 59-72.

106. Borges, J., et al., *Chorioallantoic membrane angiogenesis model for tissue engineering: a new twist on a classic model.* Tissue Eng, 2003. **9**(3): p. 441-50.

107. Di Rocco, C., G. Tamburrini, and D. Pietrini, *Blood sparing in craniosynostosis surgery.* Semin Pediatr Neurol, 2004. **11**(4): p. 278-87.

108. Namdar, T., et al., *Complete free flap loss due to extensive hemodilution.* Microsurgery, 2010. **30**(3): p. 214-7.

109. Paccagnella, F., et al., *[Autotransfusion technic in surgery of craniostenoses in children].* Minerva Anestesiol, 1989. **55**(4): p. 165-8.

110. Almeida, M.F., *Preoperative normovolemic hemodilution in aesthetic plastic surgery.* Aesthetic Plast Surg, 1999. **23**(6): p. 445-9.

111. Spahn, D.R., et al., *Use of perflubron emulsion to decrease allogeneic blood transfusion in high-blood-loss non-cardiac surgery: results of a European phase 3 study.* Anesthesiology, 2002. **97**(6): p. 1338-49.

112. Spahn, D.R., et al., *Cardiovascular and coronary physiology of acute isovolemic hemodilution: a review of nonoxygen-carrying and oxygen-carrying solutions.* Anesth Analg, 1994. **78**(5): p. 1000-21.

113. Glacet-Bernard, A., et al., *Effect of isovolemic hemodilution in central retinal vein occlusion.* Graefes Arch Clin Exp Ophthalmol, 2001. **239**(12): p. 909-14.

114. Graber, M., et al., *[Comparison of early management of central retinal vein occlusion with ranibizumab versus hemodilution].* J Fr Ophtalmol, 2015. **38**(9): p. 815-21.

115. Ahlberg, A., et al., *Preoperative normovolemic hemodilution in total hip arthroplasty. A clinical study.* Acta Chir Scand, 1977. **143**(7-8): p. 407-11.

116. Olsfanger, D., et al., *Acute normovolaemic haemodilution and idiopathic scoliosis surgery: effects on homologous blood requirements.* Anaesth Intensive Care, 1993. **21**(4): p. 429-31.

117. Singh, J., *The national centre for the replacement, refinement, and reduction of animals in research.* J Pharmacol Pharmacother, 2012. **3**(1): p. 87-9.

118. Hill, J.B., et al., *Preoperative anemia predicts thrombosis and free flap failure in microvascular reconstruction.* Ann Plast Surg, 2012. **69**(4): p. 364-7.

119. Mlodinow, A.S., et al., *Anemia is not a predictor of free flap failure: a review of NSQIP data.* Microsurgery, 2013. **33**(6): p. 432-8.

120. Nelson, J.A., et al., *Preoperative anemia impacts early postoperative recovery following autologous breast reconstruction.* J Plast Reconstr Aesthet Surg, 2014. **67**(6): p. 797-803.

121. Ness, P.M., D.L. Bourke, and P.C. Walsh, *A randomized trial of perioperative hemodilution versus transfusion of preoperatively deposited autologous blood in elective surgery.* Transfusion, 1992. **32**(3): p. 226-30.

122. Qiao, Q., et al., *Application of hemodilution in microsurgical free flap transplantation.* Microsurgery, 1996. **17**(9): p. 487-90.

123. Velanovich, V., et al., *The effect of hemoglobin and hematocrit levels on free flap survival.* Am Surg, 1988. **54**(11): p. 659-63.

124. Amoroso, M., et al., *The Effect of Normovolemic and Hypervolemic Hemodilution on a Microsurgical Model: Experimental Study in Rats.* Plast Reconstr Surg, 2015. **136**(3): p. 512-9.

125. Atchabahian, A. and A.C. Masquelet, *Experimental prevention of free flap thrombosis. II: Normovolemic hemodilution for thrombosis prevention.* Microsurgery, 1996. **17**(12): p. 714-6.

126. Farina, J.A., Jr., et al., *Comparative study of isovolemic hemodilution with 3% albumin, dextran-40, and prophylactic enoxaparin (LMWH) on thrombus formation at venous microanastomosis in rats.* Microsurgery, 2006. **26**(6): p. 456-64.

127. Farina, J.A., Jr., et al., *Effect of isovolemic hemodilution with 3% albumin on thrombus formation at venous microanastomosis in rats.* Microsurgery, 2002. **22**(4): p. 152-7.

128. Clark, E.R. and E. Linton Clark, *Microscopic observations on the growth of blood capillaries in the living mammal.* American Journal of Anatomy, 1939. **64**: p. 251-301.

129. Druecke, D., et al., *Neovascularization of poly(ether ester) block-copolymer scaffolds in vivo: long-term investigations using intravital fluorescent microscopy.* J Biomed Mater Res A, 2004. **68**(1): p. 10-8.

130. Säljö, K., et al., *Successful engraftment, vascularization, and In vivo survival of 3D-bioprinted human lipoaspirate-derived adipose tissue.* Bioprinting, 2020. **17**: p. e00065.